catalysts

MDPI

Article

Comparison of Catalysts with MIRA21 Model in Heterogeneous Catalytic Hydrogenation of Aromatic Nitro Compounds

Alexandra Jakab-Nácsa [1], Emőke Sikora [2], Ádám Prekob [2], László Vanyorek [2], Milán Szőri [2], Renáta Zsanett Boros [1], Károly Nehéz [3], Martin Szabó [3], László Farkas [1] and Béla Viskolcz [2,*]

[1] BorsodChem Ltd., Bolyai tér 1, H-3700 Kazincbarcika, Hungary; alexandra.nacsa@borsodchem.eu (A.J.-N.); renata.boros@borsodchem.eu (R.Z.B.); laszlo.farkas@borsodchem.eu (L.F.)
[2] Institute of Chemistry, Faculty of Materials Science and Engineering, University of Miskolc, H-3515 Miskolc-Egyetemváros, Hungary; kemsik@uni-miskolc.hu (E.S.); kempadam@uni-miskolc.hu (Á.P.); kemvanyi@uni-miskolc.hu (L.V.); kemszori@uni-miskolc.hu (M.S.)
[3] Institute of Information Science, University of Miskolc, H-3515 Miskolc-Egyetemváros, Hungary; aitnehez@uni-miskolc.hu (K.N.); iitszabo@uni-miskolc.hu (M.S.)
* Correspondence: bela.viskolcz@uni-miskolc.hu

Abstract: The vast majority of research and development activities begins with a detailed literature search to explore the current state-of-the-art. However, this search becomes increasingly difficult as we go into the information revolution of 21st century. The aim of the work is to establish a functional and practical mathematical model of catalyst characterization and exact comparison of catalysts. This work outlines the operation of the MIskolc RAnking 21 (MIRA21) model through the reaction of nitrobenzene catalytic hydrogenation to aniline. A total of 154 catalysts from 45 research articles were selected, studied, characterized, ranked, and classified based on four classes of descriptors: catalyst performance, reaction conditions, catalyst conditions, and sustainability parameters. MIRA21 is able to increase the comparability of different types of catalysts and support catalyst development. According to the model, 8% of catalysts received D1 (top 10%) classification. This ranking model is able to show the most effective catalyst systems that are suitable for the production of aniline.

Keywords: hydrogenation; catalyst; aromatic; nitrobenzene; aniline; data mining; quantitative comparison; catalyst ranking

check for updates

Citation: Jakab-Nácsa, A.; Sikora, E.; Prekob, Á.; Vanyorek, L.; Szőri, M.; Boros, R.Z.; Nehéz, K.; Szabó, M.; Farkas, L.; Viskolcz, B. Comparison of Catalysts with MIRA21 Model in Heterogeneous Catalytic Hydrogenation of Aromatic Nitro Compounds. *Catalysts* **2022**, *12*, 467. https://doi.org/10.3390/catal12050467

Academic Editor: Vladimir Sobolev

Received: 28 March 2022
Accepted: 19 April 2022
Published: 22 April 2022

Publisher's Note: MDPI stays neutral with regard to jurisdictional claims in published maps and institutional affiliations.

Copyright: © 2022 by the authors. Licensee MDPI, Basel, Switzerland. This article is an open access article distributed under the terms and conditions of the Creative Commons Attribution (CC BY) license (https://creativecommons.org/licenses/by/4.0/).

1. Introduction

1.1. Long-Time History, Rapid Evolution

Historically, the development of the important industrial processes required large amount of time and energy. Early designs of catalytic processes were mainly based on trial-and-error, which is solution-oriented and requires little a priori knowledge about the system itself [1,2]. Furthermore, the success of these methods are generally system-specific and probably requires further optimization. For instance, the catalytic synthesis of ammonia was first reported by Haber and further optimized by the German chemist Mittasch, who is well-known for his systematic research approach [3,4]. Mittasch et al. carried out about 20,000 tests and investigated more than 3000 potential catalysts until the optimal catalyst for ammonia synthesis was identified. Since then, more modern studies have investigated a wide range of catalysts with different instrumental analytical techniques to understand specific reaction mechanisms [5,6].

Nowadays, the success of a company also depends on fast and accurate information acquisition, continuous development, and technological innovation. The development of novel industrial processes requires data accumulation and professional data analysis that can be later turned to profit. In other words, designing a new catalyst requires a comprehensive approach [7]. It is required to know how to influence the catalytic

performance, and what kind of parameters can affect the reaction, what kind of interactions can affect these parameters [8].

The direction of catalyst development is also determined by the demands of the industry. The development of new heterogeneous catalysts is still justified, because of ever evolving approaches in industry such as environmentally friendly and economic processes.

The aim of this article is to shorten the innovation path between industrial technologies and academic research by ranking the diverse sub-research results in a uniform way. The most basic criterion for starting catalyst production is that the catalyst shows high activity under laboratory conditions. Of course, further research and development works must follow the initial laboratory tests. Many parameters need to be considered to decide which catalyst will be suitable for use in industrial setting. This is the reason why we have developed the MIRA21 model and ranking system. This work can facilitate decision-making by industry participants in catalyst development.

1.2. Data Overflow

In the last 20 years, nearly 25 million research articles have been published [7]. Not only the number of publications but also the number of patents has increased with about 700,000 published in 10 years. In the field of catalysis, the number of articles is almost 69,000 in the period 2014–2019, which is an extremely large number. Nowadays, at the beginning of a scientific work or industrial development, it is becoming increasingly difficult to review the literature of a subject area completely.

A new catalyst must demonstrate a significant improvement in yield, efficiency, selectivity, and cost effectiveness over previous methods. However, such comparisons are not straightforward. Conventional parameters such as conversion rate and selectivity are included in most publications, but even their comparison is far from trivial since catalytic attributes are generally not standardized.

Catalysis informatics deals with the extraction of knowledge from information [9], utilization of scientific publications data is still challenging due to different quality and quantity of data sets. Catalysis informatics includes Machine Learning (ML) techniques, which have been successfully utilized in various fields of scientific research [10–14] as well as in the field of catalytic reactions [15–21]. For instance, Takigawa et al. applied ML to predict how electronic and geometric structures affect the activity of heterogeneous metal catalysts [22]. Rothenberg investigated predictive descriptor modelling in heterogeneous catalysis to improve data mining [23]. In spite of this pioneering works, heterogeneous catalysis remains a major challenge for ML and data mining. Finding appropriate and exact descriptors for heterogeneous catalysis and catalysts is difficult because the activity of solid catalysts depends on a large number of variables.

Pirro et al. studied descriptor–property relationships in heterogeneous catalysis through the oxidative coupling of methane [24]. The aim of the research was to propose a method to compare the similarities between experimental data and simulated performances. The advantage of such an approach is that there is the possibility to attribute chemical meaning to the results, however small datasets were available in the case of this reaction.

This study focuses on the extraction of information from diverse, heterogeneous data. It is a preliminary investigation of a machine learning process as a manual "human learning" project with the Miskolc Ranking 21, MIRA21 model. MIRA21 is a new method to develop a more general understanding of catalytic processes from basic experimental data. The aim of the model is to characterize and qualify catalytic processes, to make the existing experimental results comparable with each other and to support catalytic development with information gained from data.

Our basic goal is to determine the parameters on the basis of which the different catalysts can be compared. By identifying these parameters, it becomes possible to standardize publication results and further use the parameter set in machine data collection.

We evaluate the model by applying it to the heterogeneous catalysis of the hydrogenation of nitrobenzene to aniline. Based on SciFinder searches [25], limiting the reaction to the

reduction of unsubstituted nitrobenzene to unsubstituted aniline by H_2 excluding patents and limiting the period from 2000 to 2021, 722 such articles where identified. If the limits are further loosened by extending the reaction to other nitroarenes, the number of articles jumps to 65,900. Nevertheless, we selected a single reaction and processed only the high quality articles in the database. The reason is that we wanted to study those articles where we have as much data as possible to set up the parameter set obviously.

In this work, we utilized 45 articles describing 154 selected catalysts and generated a data set based on 15 different descriptors and ranked the catalysts according to their generated MIRA21 number. It is not the purpose of this work to provide a complete historical overview of the specific reaction and catalysts.

1.3. Catalytic Hydrogenation of Nitro Aromatics

In order to develop a catalyst, it is essential to know the complete reaction mechanism of the reaction in question. The formation of by-products can be mapped based on the accepted reaction mechanism.

Aromatic nitro compounds are widely used in explosives, pesticides, fertilizers, dyes, pharmaceuticals, plastics, resins, and fuel additives. The growing demand of these industry sectors have an effect on the nitro aromatics market, especially that of nitrobenzene, which was valued at USD 9.3 billion in 2019 [26,27].

The hydrogenation of aromatic nitro compounds is widely studied [8,28–30]. Nitrobenzene is the raw material of aniline production [31]. The Bechamp reduction of nitrobenzene is the oldest technical process of aniline synthesis, which uses iron in the presence of hydrochloric acid [32] while the modern processes of industrial aniline production is carried out by the catalytic hydrogenation of nitrobenzene in gaseous or liquid phases and in the presence of metal catalysts [33,34]. The following reaction equation shows the general reaction of the hydrogenation of nitrobenzene to aniline (Figure 1).

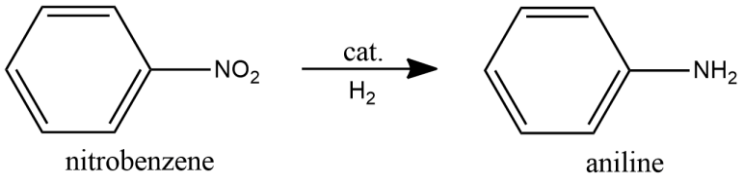


Figure 1. General reaction of nitrobenzene hydrogenation to aniline.

Industrial catalysts consist of a catalyst carrier and one or more hydrogen activating metal. Although, the effect of various catalyst carriers, whether in monometallic or bimetallic systems, promotors and different technological process steps and conditions have been described, and only a few publications provide direct comparisons with other studies [35,36].

Haber published the first scheme of the hydrogenation of nitrobenzene at the end of 19th century [35]. He proposed a three-step process for the formation of nitrobenzene to aniline. Although the reaction mechanism was widely accepted, several studies were later carried out to understand the process in greater detail [37–39]. Later, Gelder et al. brought forward a new mechanism following a detailed analysis of the surface reaction mechanism [40]. Figure 2 shows the difference between the Haber and Gelder mechanisms. According to the Gelder concept, Ph-N(OH) is a common intermediate in the hydrogenation reaction and it can directly react with an adsorbed hydrogen to produce Ph-NH and finally the aniline product. In addition, Ph-N(OH) reacts with itself and produce azoxybenzene.

Mahata et al. have investigated direct and indirect pathways of nitrobenzene by density functional theory calculations to understand the underlaying reaction mechanism [41]. The direct pathway involves the reduction of nitrobenzene to aniline through nitrosobenzene and hydroxylamine intermediates. In the indirect pathway these intermediates condense to form the azoxybenzene intermediate. Aniline was formed by hydrogenation of azoxybenzene and subsequent cleavage of the *azo* bond. Based on their calculations

they found that the direct reduction pathway of nitrobenzene over Ni(111) catalyst is more favorable than the indirect pathway.

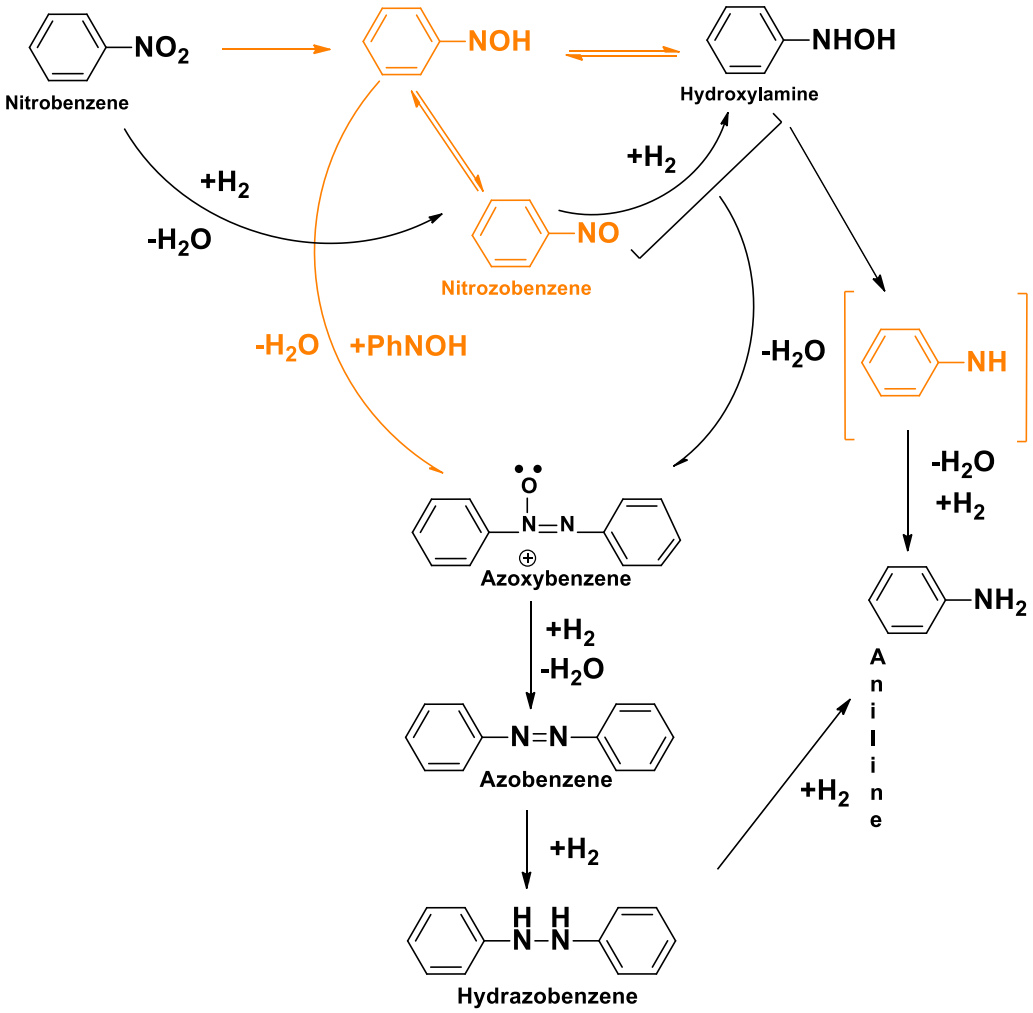


Figure 2. Possible reaction pathways of the hydrogenation of nitrobenzene to aniline. Presentation of Haber (black) and difference by Gelder (orange) mechanism.

The possible by-products in the catalytic hydrogenation of nitrobenzene are also relatively well-known. Therefore, we chose this reaction to develop MIRA21 model.

2. Methods—MIRA21 Model

2.1. Descriptor System

The methodology of Miskolc Ranking 2021 (MIRA21) is a multi-step process for identifying novel, potentially useful, and interpretable patterns in data collected for the catalytic hydrogenation of nitrobenzene. The main steps for this Knowledge Discovery in Databases (KDD) [42] approach are shown in Table 1.

The main purpose of the MIRA21 model is to provide a standard to characterize the "goodness" of a catalyst with objective numerical data, and to compare and rank the catalysts accordingly. Characterizing and ranking the catalysts will promote the efficient selection of the relevant properties to support the design of a new catalyst or to improve existing ones. The comparison of special catalysts for a reaction enables research and development trends to be monitored. The standardization of the accessible data in MIRA21 also promotes accurate, consistent, and uniform data in future publications.

Table 1. Steps for establishment of MIRA21 model as a process of Knowledge Discovery from Data.

Identification the aim of KDD	**1**	**Identification of the aim of MIRA21 and the application domain**
Creating target data set	**2**	Determination of primary selection criteria of scientific publications
Data cleaning	**3**	Filter out of journal articles that does not complying with the terms
Data integration	**4**	Creating MIRA21 data warehouse
Data selection	**5**	Selection of useful attributes to characterize catalytic performance
Data transformation	**6**	Transforming of data into forms appropriate for data mining
Data mining	**7**	Searching for patterns from data set of catalysis database
Pattern evaluation	**8**	Determination of catalyst ranking and development directions
Knowledge presentation	**9**	Documentation and reporting discovered knowledge in a review article

MIRA21 contains data extracted from 45 articles on the catalytic hydrogenation of nitrobenzene [34,36,43–84].

Figure 3 shows the formation of the MIRA21 number that was assigned to each catalyst. In addition, this number provides two other indices. The subscript presents the number of studied parameters and the superscript shows that how many attributes can be found in the scientific publication (number of known parameters). These two metrics provide additional information about the amount of available published data. If only a few known parameters are in a publication, the characterization of the catalyst according to the MIRA21 model will be less robust. The HNB (**H**ydrogenation of **N**itro**B**enzene) acronym shows the types of catalytic reaction. D1 classification corresponds to the top 10% of the catalysts. Quartiles were also defined, wherein the four quartiles: Q1 (first quartile), Q2 (second quartile), Q3 (third quartile), Q4 (fourth quartile) were used.



Figure 3. Quantitative description of a catalyst by MIRA21 number with corresponding classification and color code: D1 (top10%) = linen, Q1 (0–25%) = apricot, Q2 (25–50%) = light orange, Q3 (50–75%) = mint, Q4 (75–100%) = turquoise.

As there is no exact data on which parameters affect the performance of a catalyst and how it does so, we must therefore identify an arbitrarily weighted descriptor system. Selection of descriptors was based on previous knowledge and our experience in literature search. On the one hand, there are properties that clearly characterize a given catalyst. On the other hand, it is foreseeable that scientific publications contain only a limited range of data.

The descriptor system of the model can be divided into four classes, as shown in Table 2. The quantifiable classes are the catalyst's performance, reaction conditions, and catalyst conditions. The sustainability parameters comprise the non-quantifiable class. Our model applies different weighting to different classes. In the first step we determined an initial weighting of the four classes. The purpose of the weighting method is to provide a usable numerical value that also differentiates the four classes with the least distortion.

The first class characterizes the catalytic performance on a scale from 1 to 10, with 10 being the highest performance. The second class of parameters of the reaction conditions are temperature, pressure, time, and the quantities of the initial materials. We considered them 50% less in weight compared to the first class. The third class consists of the catalyst's physical parameters. These parameters are given 80% less weight than the first class. The fourth class pertains to sustainability. The vast majority of scientific publications do not include studies on sustainability, despite the fact that this is one of the most burning issues

in our days. This is the reason why we considered this class with greater weighting than the third class, thus supporting the importance of sustainability.

Table 2. Descriptor system of MIRA21 model.

			Test Parameters				Scoring	
	Categories	No.	Notation	Name	Unit	Definition	FROM	TO
Quantifiable parameters	I. Catalyst performance	1.	X_{NBmax}	Maximum conversion Equation (1)	mol%	Maximum nitrobenzene conversion achieved on a given catalyst	1	10
		2.	Y_{AN}	Aniline Yield Equation (2)	mol%	Aniline yield for maximum conversion	1	10
		3.	S_{AN}	Product Selectivity Equation (3)	mol%	Aniline selectivity for maximum conversion	1	10
		4.	TON_{AN}	Turnover Number Equation (4)	-	Number of moles of aniline formed per 1 mol active metal when the maximum conversion reached	1	10
	II. Reaction conditions	5.	$T_{max.conv.}$	Temperature	K	Reaction temperature for maximum conversion	2.5	7.5
		6.	$P_{max.conv.}$	Pressure	atm	Reaction pressure for maximum conversion	2.5	7.5
		7.	$t_{max.conv.}$	Time	min	Time required to reach maximum conversion	2.5	7.5
		8.	$n_{cat.}$	Molar amount of initial catalyst	mol	The molar amount of the active metal involved in the reaction—in case of several metals, the sum of molar numbers	2.5	7.5
		9.	n_{NB}	Molar amount of initial nitrobenzene	mol	The initial amount of nitrobenzene involved in the reaction	2.5	7.5
	III. Catalyst conditions	10.	CPZ	Catalyst Particle Size	nm	Average particle size of the catalyst	4	6
		11.	CSA	Catalyst Surface Area	m^2/g	Catalyst (active metal + support) surface area	4	6
				Does the publication contains information about these subjects?			MIN	MAX
Non-quantifiable parameters	IV. Sustainability parameters	12.	Rea	Information about Reactivation	-	Reactivation means the physical process by which the activity of the catalyst used returns to or near the original activity level.	2.5	7.5
		13.	Stab	Information about stability of catalyst	-	Stability means preservation of catalytic activity	2.5	7.5
		14.	Care	Information about catalyst carrier effect	-	Carrier effect means that the catalyst support influences the catalytic reaction	2.5	7.5
		15.		Catalyst carrier effect	-	Nature of the effect (positive, no effect, negative)	2.5	7.5

At first, 20 descriptors have been defined to evaluate the performance of each catalyst. Based on the findings of the literature search, the number of descriptors was reduced to 15. The present study does not attempt to examine the interdependence of the parameters on each other. Table 2 shows the descriptor system of the 15 parameters, with their notation, unit, definition, and weighted scoring.

During data processing, we encountered three types of data. The first data type provides explicit information on the attribute, which is called the available data. The second is derived data, which can be calculated from known information. The third is graphical data, which is called readable data. Derived and readable data are also marked in the data set. The calculations were performed in a predetermined way. The Origin program was used to read the figures of journal articles [85].

The maximum conversion, X_{NBmax} % obtains the highest priority in the data analysis. All additional data depend on the conversion. The determination of the maximum conversion is based on the following equation (Equation (1)):

$$X_{NBmax} = \frac{consumed\ n_{nitrobenzene}}{initial\ n_{nitrobenzene}} \times 100 \quad (1)$$

The following equation was used to calculate the yield of aniline, Y_{AN} (Equation (2)):

$$Y_{AN} = \frac{synthetized\ n_{aniline}}{theoretical\ n_{aniline}} \times 100 \quad (2)$$

The aniline selectivity, S_{AN} of the catalyst was calculated as follows (Equation (3)):

$$S_{AN} = \frac{synthetized\ n_{aniline}}{consumed\ n_{nitrobenzene}} \times 100 \quad (3)$$

where $n_{aniline}$ and $n_{nitrobenzene}$ are the corresponding molar amounts of the compounds.

Conversion, yield, and selectivity are required to describe catalytic performance can generally be found using a literature research. Publications usually contain just some of these three data types or pairs of them. Therefore, we increased the weighting of catalyst performance in the ranking by using all three attributes, although their independence was not examined.

There are several publication about the explanation of TOF (turnover frequency) and TON (turnover number) [86–88]. Study of Kozuch et al. wrote a detailed discussion about the definition and application of these metric and using TOF in connection of heterogeneous catalysis [88].

Although Boduart created the first definition of turnover frequency in the 1960s [89], the use of TOF and TON numbers is still varied in heterogeneous catalysis. Literature experience has shown that these metrics are used in a variety of ways to communicate the results of scientific research. We found most of the data as TON number in articles.

For standardization of data, we determined a TON number based on the definition as follows: "turnover number specifies the maximum use that can be made of a catalyst for a special reaction under defined reaction conditions by the number of molecular reactions or reaction cycles occurring at the reactive center up to the decay of activity" [90].

According to this explanation, the following equation (Equation (4)) was used to calculate the turnover number of aniline, TON_{AN}:

$$TON_{AN} = \frac{synthetized\ n_{aniline}}{n_{catalyst}} \quad (4)$$

where $n_{catalyst}$ is the corresponding molar amount of catalytically active metal.

We found catalysts that were tested in a tubular reactor. In cases where we could not clearly determine the residence time, we took the data uniformly for 60 min. These cases were marked with "*" in the data set.

The second class consists of data about the reaction conditions: reaction temperature, reaction pressure, reaction time to reach maximum conversion, the molar amount of the catalyst, and the molar amount of the initial nitrobenzene. In industrial processes, the hydrogenation of nitrobenzene is carried out at elevated temperatures and pressures. However, in MIRA21 model, temperature and pressure were scaled and scored from a

thermodynamic economics point of view. The higher the temperature and pressure, the more expensive the reaction is from an energetic point of view. In cases where we found more than one maximum conversion data, the second priority was reaction time. The calculation of molar amount of the catalyst was defined as the molar amount of active metal involved in the reaction. In cases where two or more active metals were used, the total amount of catalyst is the sum of the molar amounts.

The third class of attributes is the particle size and catalyst specific surface area. It is important to note that these parameters apply to the prepared catalyst, as the surface areas of the catalyst and the support are different.

Normally, there is a clear relationship between particle size and specific surface area [91–93]. The optimal surface area to which the reactant can contact varies from reaction type to reaction type. Thus, it is useless to increase the specific surface area if the reactant is inaccessible. This is the reason why we have included both properties in the descriptor system. On the other hand, particle size can be a determining parameter not only for the reaction but also for the separation technique from an industrial point of view. Particle size distribution is another key parameter for catalyst characterization [94–96]. However, we removed the particle size distribution from the descriptor system, due to the lack of data or its lack of consistent and uniform application.

The last section of the descriptors contains the non-quantifiable parameters. The aim of these descriptors is the investigation of catalysts from a sustainability point of view. Almost all of the studied catalysts were self-produced, therefore they are not commercially available. Economic and environmental sustainability considerations also arise when examining the suitability of a catalyst. Although, there can be several indicators of sustainability, the descriptors are dictated by the data available in publications. We included data about reactivation methods, the stability of the catalyst, and catalyst carrier effect.

The data collected must be transformed into forms that are appropriate for data mining. Our goal was to carry out as few data transformations as possible to reduce the distortion of the results. In the first step, we classified the descriptors in four classes. These parameters were rescaled according to the scoring.

The following equation was used to normalize the data from quantifiable parameters (Equation (5)):

$$A^t = MIN + \frac{(MAX - MIN) \times A - min_A}{max_A - min_A} \quad (5)$$

where A is the value of the attribute, A^t is the transformed attribute value, min_A and max_A are the corresponding calculated minimum and maximum values of the attribute in the data set, MIN is the minimum scoring point, and MAX is the maximum scoring point. As the data sets changes, the minimum and maximum values of a given attribute also change, which means that scaling depends on the current data set. Outliers also can affect remarkably the scaling and scoring system.

Frequently, the values of conversion, yield, and selectivity were given inaccurately. Authors often use the context of "above 99%" or "more than 99%" to characterize catalytic performance. That is why we made no distinction between 99% and 100% and we gave a maximum score to conversions for values of 99% or above.

Non-quantifiable data were scored at 2.5 or 7.5 points, except carrier effects. In case of carrier effects, we also examined the nature of the effect. If the studied catalyst carrier had a positive effect on catalytic performance, it got 7.5 points. If the catalyst support has no effect on the reaction, it received 5 points. The catalyst that negatively affected the hydrogenation reaction, received 2.5 points.

The normalized data were summed in a multiplication function and we took its respective logarithm to the base ten. The following equation shows the formulation of the MIRA21 number (Equation (6)):

$$MIRA21 = log \prod_{i=1}^{n} A_i^t \quad (6)$$

where $i = 1 \ldots 15$ is the number of attributes, and A^t is the transformed value of an attribute between the corresponding scores. The value can be specified with a decimal point due to the logarithmic calculation. However, the second decimal point was also indicated in the tables of ranked catalysts because of ranking clarification.

Each catalyst can be characterized by MIRA21 having a maximum value of 13.43. The ranking is based on the calculated MIRA21 numbers. In addition to establishing the ranking, the results were divided into quantiles. The quantiles and its color code are shown in Table 2. The upper limit of the D1 class score was calculated by the following equation (Equation (7)):

$$Scorelimit of D1 class = MAXrank - \left(\frac{MAXrank - MINrank}{10} \right) \quad (7)$$

where $MAXrank$ is the highest and $MINrank$ is the lowest score of MIRA21 ranking. The D1 class contains catalysts that received higher than 11.7 points. Quartiles were also defined according to this principle, wherein the first decile and four quartiles: D1, Q1, Q2, Q3, Q4 were used. The first quartile is made up of Q1 and the top 10% (D1).

2.2. Database

The first step of creating the data set is to determinate the selection criteria of the journal articles for the set. The selection and data processing of journal articles were carried out by three curators according to the selection criteria. Two independent curators studied each article. When a consensus is reached between the two curators, the final data collection takes place. In case of disputed data, we discussed the data entry with the involvement of several PhD students.

The primary criteria related to the Q index is the quartile score of a journal. We only considered articles that had Q2 or Q1 index in 2019 according to the Scimago Journal & Country Rank website [97]. Furthermore, another selection criteria was that the journals must have been published after 2000. As shown in Figure 4, 86% of processed scientific publications got Q1 qualification and most of the articles were published after 2010. The keywords used to search for articles were nitrobenzene, catalytic hydrogenation, aniline, and catalyst.

The next step was to clarify data sets of the articles. From this point on, exactly what kind of data we aim to collect (secondary selection) becomes important. In the vast majority of articles, we found the data that was necessary to compile the database. Articles that did not examine nitrobenzene hydrogenation in our aspect or did not contain explicit data were omitted. During the literature search, we studied the research results of the last 20 years and found more than 100 articles in this topic.

The further step through data mining is the integration of data, data selection, and data processing. We created a *data warehouse* of journal articles and their contents. The data collected can be divided into three groups: data about the literature source, the catalyst, and the MIRA21 descriptors.

Most of the studied catalysts consist of a catalyst carrier and one or two active metal components. If we further examine the input data, variability in the composition of catalysts can be observed, as shown in Figure 5. Carbon-based supports are typically used as catalyst carriers. Although, it is hard to categorize the supports, it can be stated that most of the supports are activated carbon due to its low cost, its high capacity for the removal of organic components, and its ability to be reactivated and reused [63]. Iijima and Ichihashi, and Bethune et al. discovered carbon nanotubes (CNTs) independently in the early 1990s [98,99]. Several studies have shown that reactions can be catalyzed by CNT-supported metal catalysts [100]. Recently, more research has focused on the application of carbon nanotubes in the reactions of aromatic nitro compounds [101–103]. Moreover, various metal oxides have been used in hydrogenation reactions. Most experiments also involved silica-based carriers.

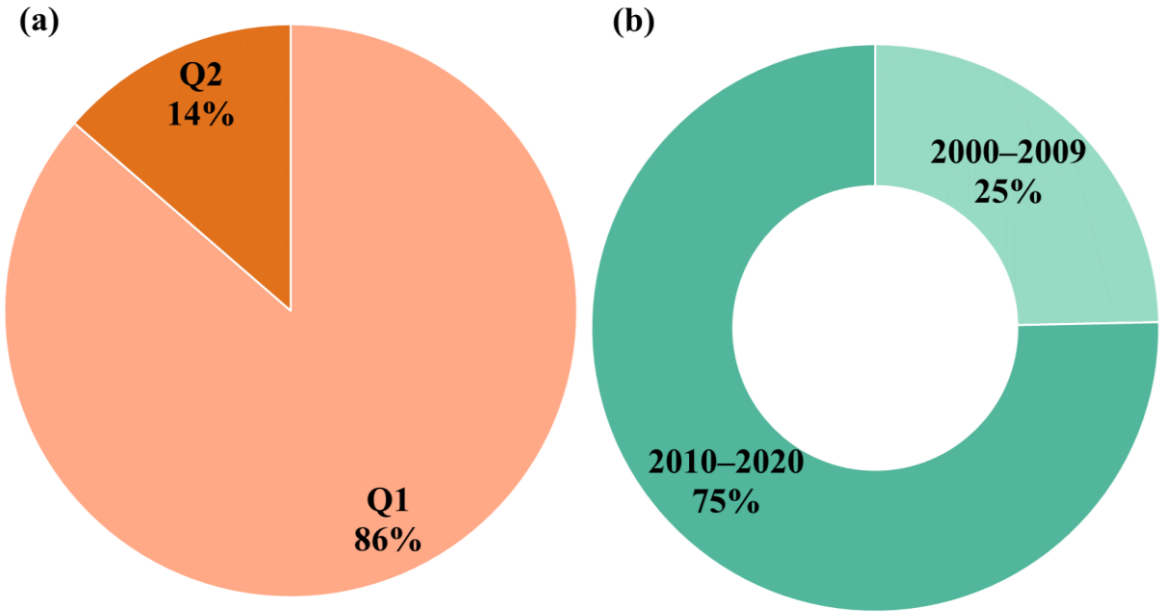


Figure 4. Statistics of studied articles: distribution of articles according to Q-index (**a**) and publication year (**b**).

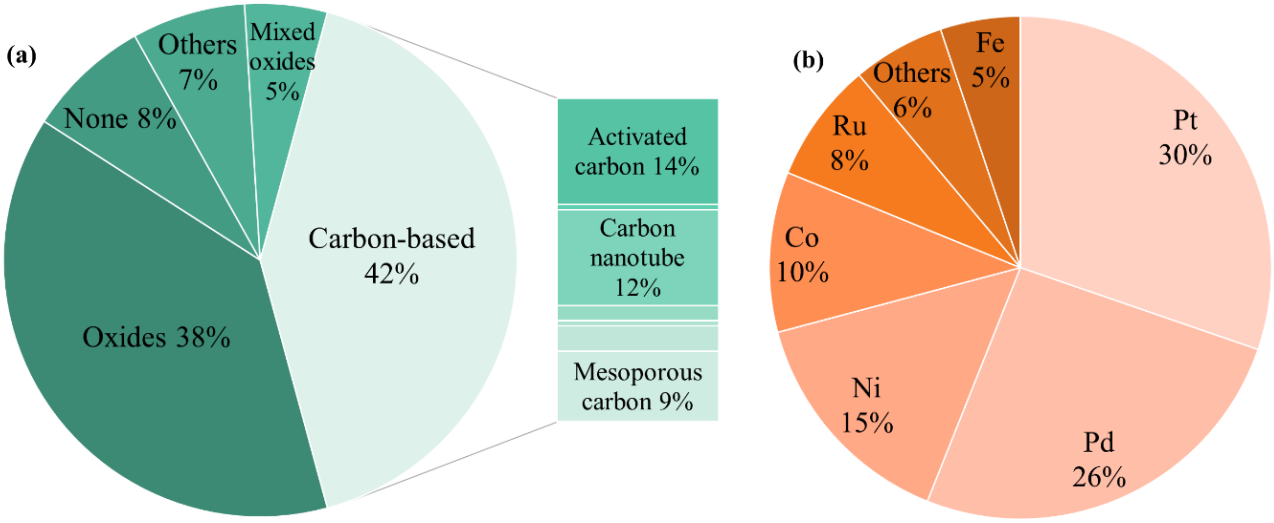


Figure 5. Distribution of catalyst carriers (**a**) and primary active metals in catalyst studies (**b**).

About 85% of catalysts were monometallic, whereas 15% of catalysts consisted of two active components. A large percentage of prepared and applied hydrogenation catalysts contained palladium or platinum as an active metal. Much research has also been performed with Ru, Rh, Co, Fe, Au, and Cu as catalysts. The distribution of the active metals was slightly distorted. The occurrence of an active metal increased not only with the number of articles but also with the number of catalysts tested in it.

The last steps of knowledge discovery (referred to in Section 2.1.) are detailed in the Results and Discussion, Overall ranking, and Conclusion sections. Data mining corresponds to the search of patterns from the database and carrying out the ranking of the catalysts.

3. Results and Discussion

We evaluated 154 catalysts of 45 different scientific journals using 15 descriptors during the literature search. Information regarding the content of the articles is illustrated in Figure 6.

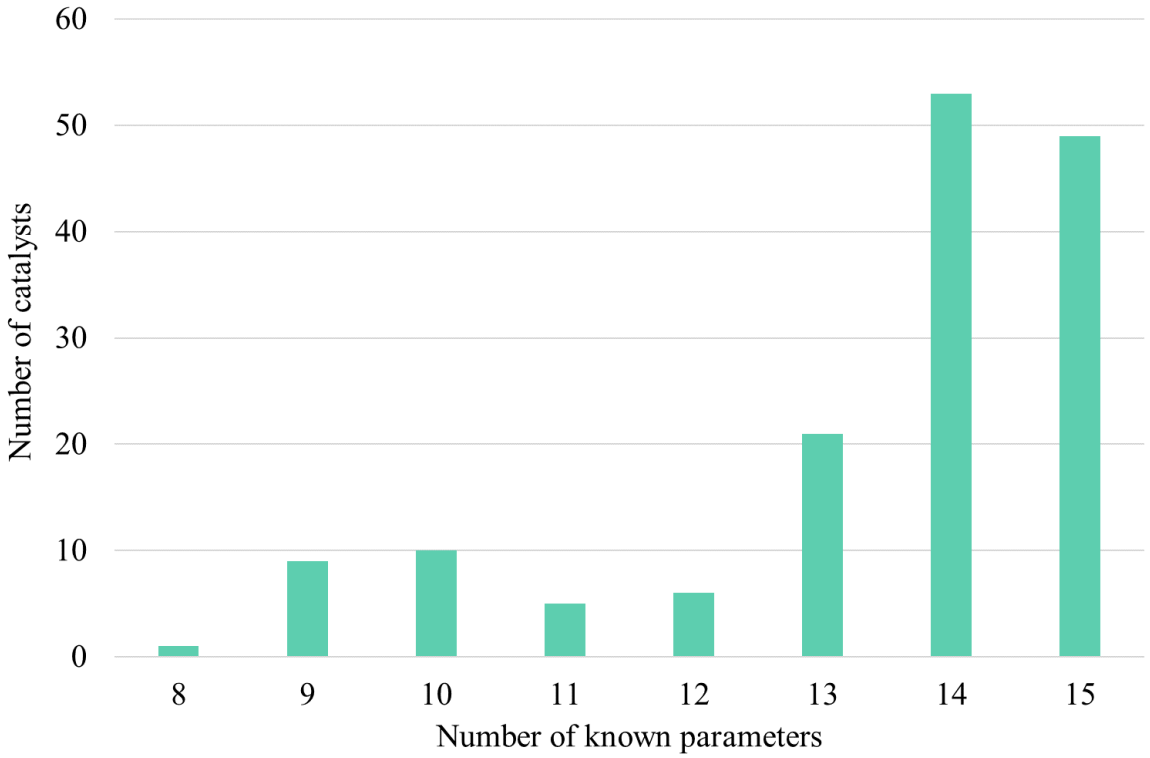


Figure 6. Information content of studied scientific publications.

Based on the diagram, the selected parameters are suitable for comparing the characteristics of the catalysts. In 80% of cases, at least 13 pieces of information were available. It is necessary to note here that not all catalysts were characterized in detail within a given article. This suggests that only the most effective catalysts were analyzed or described in detail.

Figure 7 shows the percent of data that was available for each catalyst descriptors. More than 90% of catalysts were characterized by their maximum conversion rate and selectivity. In most cases, the product yield had to be calculated. Therefore, the reason why the yield descriptor was available at such a high percentage is that the data needed for the calculation were readily available. Two indispensable characteristics of chemical reaction conditions are temperature and pressure. These metrics are always present in scientific publications, as they were in our case as well. However, no reaction time was reported in several instances. In these cases, the conversion rates and selectivity data were also either missing or there was not enough data to compute them (i.e., as in flow reactor systems). More than 90% of molar amounts of catalysts were available from the articles or could be derived from other data. An interesting observation was that there were some cases where we could not calculate the molar amount of the catalysts because the requisite data were not clearly presented. Moreover, in some experiments, the initial molar amount of the substrate was so low that the reaction performance was difficult to interpret.

A small amount of information was available on the physical properties of the catalysts. The most frequently applied analytical measurements were Brunauer–Emmett–Teller (BET) method and scanning electron microscopy analysis. The selected physical parameters were often not found in the articles.

According to the data analysis, we found that the distribution of data by catalytic performance descriptors varies (Figure 8). The next box-and-whisker chart shows the minimum, maximum, Q1–Q3 range (containing the Q1–Q2–Q3 quartiles), median values of the conversion, yield, and selectivity values. The central black line shows the median. The ends of the vertical black lines show the minimum and maximum values of each attribute.

The solid column shows the first quartile, the striped column shows the third quartile. The meeting of solid and striped columns shows the median value.

The conversion and yield values range from 1–100%, but the selectivity ranges from 32–100%. From the graph, it can be seen that the studied hydrogenation catalysts operate with high selectivity. An important point is that the range of the conversion results between Q1 and Q3 is relatively large. However, selectivity has a Q1–Q3 range between 92% and 99%. The distribution of the aniline yield is similar to the distribution of the conversion rate. Catalysts that worked with low conversion rates or aniline yields received low scores. As the first class of descriptors get the highest weighting, catalysts with low catalytic performance values are placed at the end of the ranking. The highest TON was about 35,000 and the lowest was smaller than one. The reason of the big difference is the varying amount of catalyst used in the test hydrogenation experiments.

As shown in Figure 9, the catalysts used for hydrogenation were used in a wide range of temperatures. Compared to industrial reaction conditions, laboratory experiments are typically performed at lower temperatures. While the catalysts were tested at an average temperature of 90 °C, the temperature of industrial aniline production is usually between 200 and 300 °C.

The typically used reaction pressure was less than 16 atm in case of the nitrobenzene hydrogenation in laboratory conditions. In our database, there is an outlier in terms of pressure. Zhao et al. investigated the hydrogenation reaction in supercritical carbon dioxide [78]. They examined the influence of pressure, solvent, and particle size for the Pt/C-catalyzed hydrogenation of nitrobenzene. It was shown that the conversion increased as the CO_2 pressure increased to 10 MPa, but decreased at pressures higher than 14 MPa.

The reaction time of test experiments also varied greatly. In some catalyst tests, the hydrogenation time was several hours. The reason for the multiple-hour observations could primarily be to achieve maximum conversion, and that the conversion increased over time. The shortest reaction time was 7 min in the case of a carbon-nanotube-based platinum catalyst.

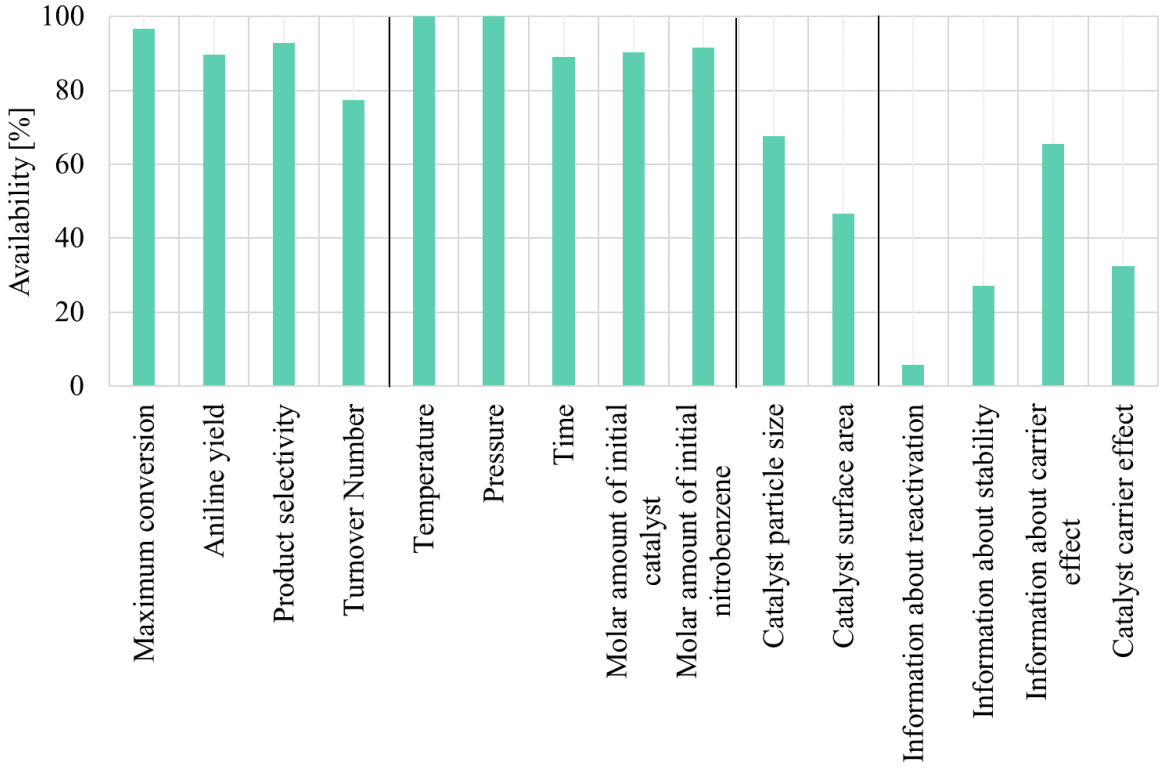


Figure 7. Relative frequency of data occurrence according to MIRA 21 descriptors.

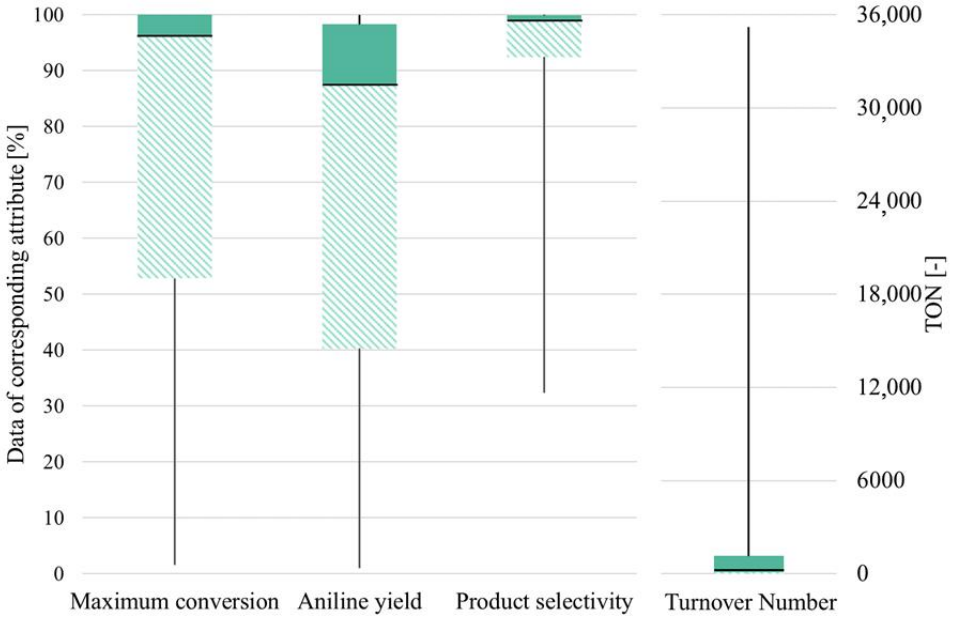


Figure 8. Availability of catalyst performance data on a box and whisker chart: maximum conversion, aniline yield, and selectivity data in percentage (**left**), TON [–] (**right**). On each box plot, the central black line indicates the median, and the solid part of the column shows the first quartile, and the striped part shows the third quartile.

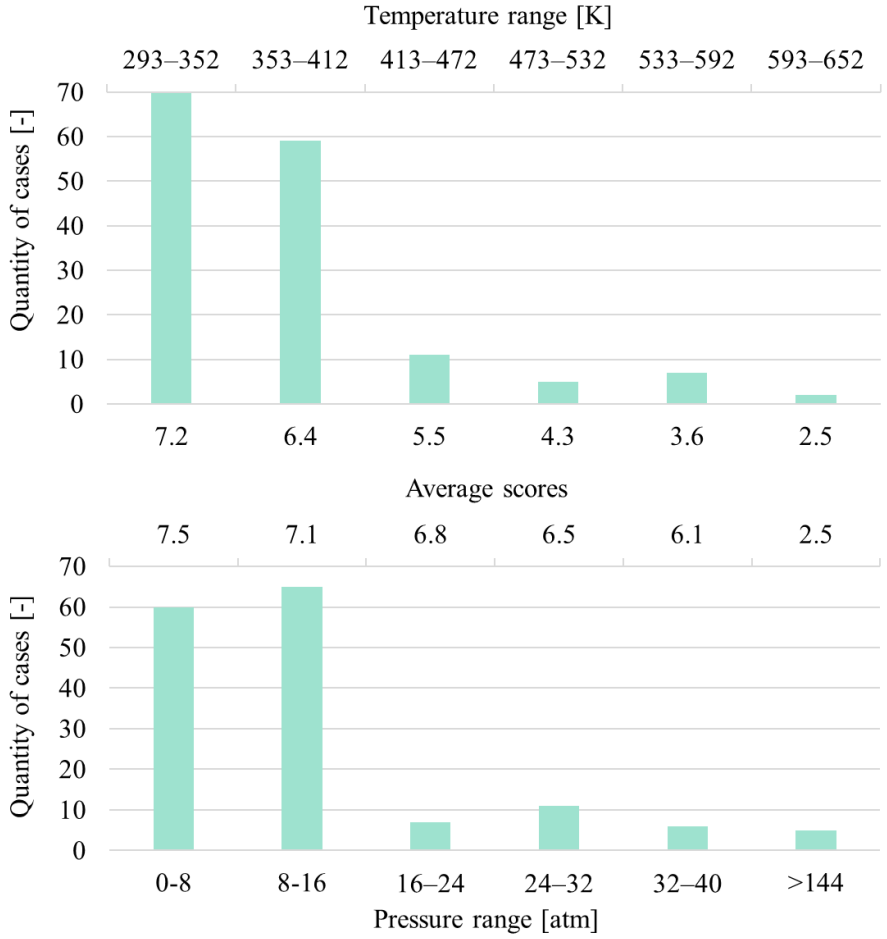


Figure 9. Values of applied reaction temperature (**top**) and pressure (**bottom**) divided into ranges. First *x*-axis shows the ranges and the second *x*-axis shows the average scoring of ranges in MIRA21.

The last descriptor evaluated the sustainability of the catalysis. These questions could be answered for all catalysts. The catalysts that were examined in terms of reactivation, stability, and catalyst support, were given a "+" rating. Furthermore, the catalyst whose support favored the reaction received an extra "+" rating.

The descriptor of reactivation defined the physical techniques, but the regeneration processes, which involve chemical treatment, were also included due to data analysis experience. Zhang et al. investigated the stability of cobalt catalysts, as well as their ability to be recycled [77]. After each reaction, the catalysts were washed with ethanol and subsequently dried. The catalyst was reused at least five times without any loss of activity. In a publication about cerium-based catalysts, centrifugation was used to separate the catalyst in order for it to be reused [62].

The stability was reported in 27% of the sampled articles; an important requirement for the catalyst to have a long lifetime. During a stability test, the number of cycles the catalyst performs before the activity of the catalyst begins to decrease was determined. In articles where several catalysts were tested, only the best of these catalysts were examined or described for stability. This could be one reason for the low amount of data on this topic. We encountered with context stability as recyclability or reusability of a catalyst in the articles. For example, Qu et al. investigated the stability of $AuPd/TiO_2$ catalysts for the solvent-free hydrogenation of nitrobenzene to aniline [79].

In many cases, the focus of articles was on the effect of the catalyst support. In a high percentage of the studies, the catalyst carrier was the novelty of the catalyst. For the reaction of nitrobenzene hydrogenations, researchers used various types of supports, including conventional carbon-based supports, carbon nanotubes, cerium oxide, and porous organic polymers. Gao et al. prepared different types of Co-based, nitrogen-, sulfur co-doped carbon hybrids for catalytic hydrogenation and studied the role of the cobalt salt [55]. They found that these catalysts could effectively reduce functionalized nitro aromatic compounds to the corresponding amines.

4. Overall Ranking

After preparation of the database, the MIRA21 ranking system was implemented. The scaling of data was done according to data-normalization. Modifications to the scaling are already included in the method description.

If we examined the occurrence of data according to the descriptors, information about reactivation, stability, catalyst surface area, carrier effect, and catalyst particle size were the least available. This experience correlates with the scoring of descriptors, except in the case of the last class of descriptor, but this was deliberate. We expected that these parameters could be used to differentiate the catalysts. This is the reason for the greater weighting of the sustainability questions.

To provide evidence to our previous statement, Figure 10 highlights one of the bases of the MIRA21 number. The more information given about a particular catalyst, the higher the MIRA21 number the catalyst could be assigned to. In addition, as the amount of data on the catalyst increases, the difference between the MIRA number of the catalyst increases, too. The reduction in the number of parameters was also examined. If we reduced the number from 15 to 10, we got a much more blurred picture on the relative quality of the catalysts.

Figure 11 shows the distribution of the catalyst classifications. The total Q1 is made up of the Q1 and D1 categories. According to the MIRA21 model, 12 catalysts were placed in the D1 category. A total of 60 of the 154 catalysts were placed in the first quartile and 16 were placed in the last quartile.

The MIRA21 number, classification, reference, catalyst ID, and catalyst name are given in Tables 3–6. Catalyst ID consists of reaction type, author address ID, year of publication, and the serial number of the catalyst. This section details the scientific research in category D1. Articles describing catalysts classified as D1 were published between 2013 and 2021.

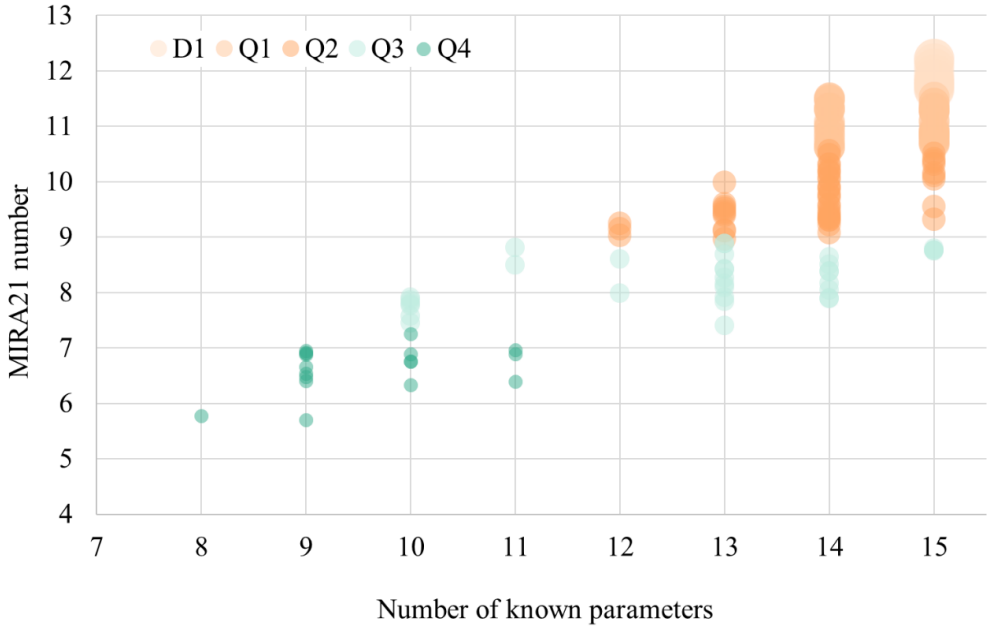


Figure 10. Effect of increasing number of known parameters for MIRA number.

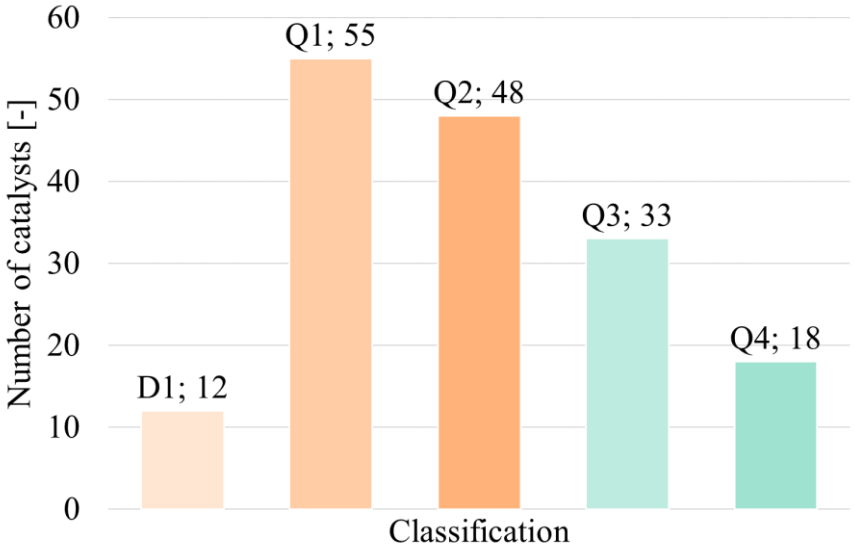


Figure 11. Distribution of catalysts according to classification (D1, Q1, Q2, Q3, Q4) system.

Table 3. Identification of D1 classified catalysts according to MIRA21 model.

RANK	CATALYST ID	CAT. Name in Journal	Reference	KNOWN Parameters	MIRA21 Number	Class.
1	HNB_XIA2021_1	0.07%Pt/@-ZrO_2/SBA-15	[36]	15	12.22	**D1**
2	HNB_BRA2015_1	Pd/C	[34]	15	12.22	**D1**
3	HNB_TAI2017_3	Co@NMC-800	[77]	15	12.13	**D1**
4	HNB_MIS2019_1	Pd/N-BCNT	[64]	15	12.04	**D1**
5	HNB_SHA2015_1	Pt/CMK-3	[66]	15	11.92	**D1**
6	HNB_MIS2020_1	5 w/w% Pd-CC	[50]	15	11.84	**D1**
7	HNB_SHA2020_1	Pt/meso-Al_2O_3	[44]	15	11.83	**D1**
8	HNB_BEI2013_2	Pd/MWCNT-SA-4.3	[73]	15	11.79	**D1**
9	HNB_GUA2017_4	Pd/N@CNTs-1.5 h	[59]	15	11.77	**D1**
10	HNB_GUA2020_2	Pt CeO_2-R-600	[62]	15	11.72	**D1**
11	HNB_HAN2013_1	Pt@MIL-101	[65]	15	11.69	**D1**
12	HNB_LAN2020_3	γ-Fe_2O_3/NPC-800	[84]	15	11.65	**D1**

The highest scoring monometallic catalysts contained either palladium or platinum as the active compound. Figure 12 shows the distribution of the active compound and type of catalyst carriers in each case of the D1 catalysts. In the case of active metal, the distribution is similar to that in category Q1, but the percentages of palladium and platinum are reversed (42% platinum and 35% palladium). Overall, this highlights that either palladium or platinum should be used to catalyze the production of aniline by hydrogenation. Given that palladium is much more expensive than platinum, it is worth considering the further development of platinum catalysts. Researchers also applied various special catalyst supports. The latest nitrobenzene hydrogenation research were performed with carbon-nanotube-based catalysts, but there are several special solutions of support compounds.

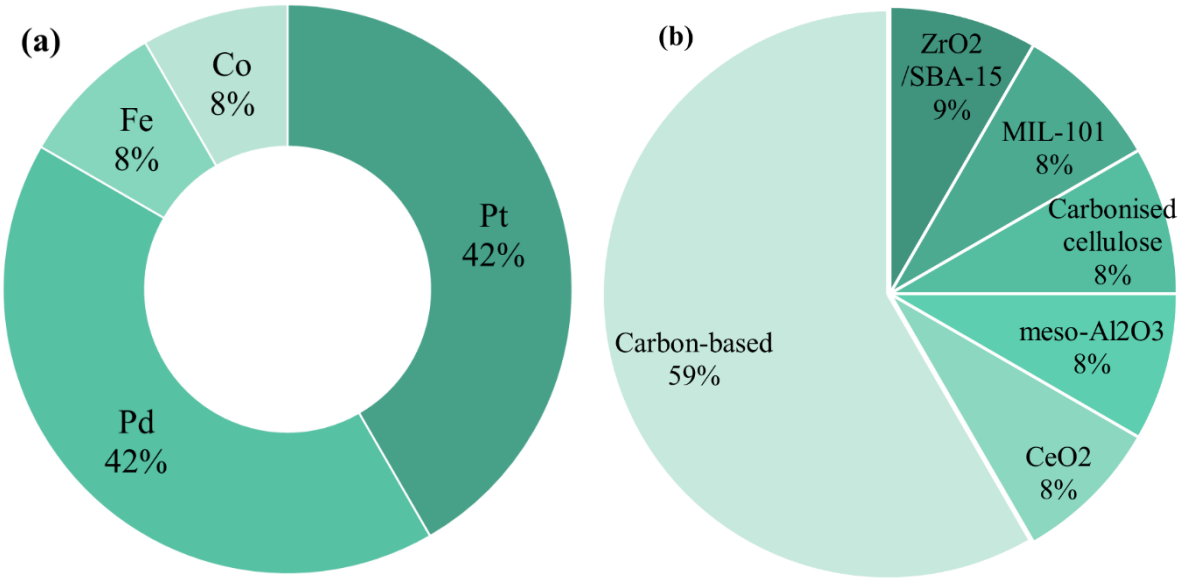


Figure 12. Distribution of active metals (**a**) and type of catalyst carriers (**b**) in D1 classified catalysts.

After scoring of the descriptors, there was no significant difference in catalytic performance. The experiments occurred at the temperature range of 20–80 °C. There were much larger differences in the reaction pressures. The ranking of D1 classified catalysts was most affected by the turnover number. However, there were also large differences in the professional information content of articles, whether they investigated reactivation, regeneration, support effect, or stability.

Y. Zhang et al. prepared hybrid 0.07% Pt/@-ZrO_2/SBA-15 nanostructure catalyst which demonstrated 100% conversion and 100% aniline selectivity at 40 °C, 7 atm in 50 min [36]. The high activity, selectivity, and stability of the catalyst can be attributed to the special structure of the catalyst and the synergistic effect within it. The authors compared this catalyst to many other catalysts from different studies.

Research of Turákova et al. focused on the mechanism of the liquid phase hydrogenation of nitrobenzene [34]. They used a conventional palladium catalyst with activated carbon support. At 70 °C and 30 atm, the nitrobenzene conversion was almost 100% after 40 min. This high pressure is commonly used in industrial applications.

The D1 category of MIRA21 also includes non-noble metal catalysts for nitrobenzene hydrogenation. It should be noted that most of the hydrogenation catalysts developed contain precious metals. In contrast, researchers from Taiwan developed a Co-based N-doped mesoporous carbon catalyst that demonstrates high catalytic activity and chemo selectivity for various nitro aromatics at 80 °C and 1 MPa with only 2 mol% of cobalt [77]. The synthesis of the catalysts facilitate the simultaneous optimization of porous features and cobalt nanoparticles. F. Zhang et al. have developed a new approach to improve the

catalytic activity by the formation of an embedded cobalt-based catalyst with N- doped mesoporous carbon.

Another new trend in hydrogenation catalyst development is the "support on support" (SoS) type catalyst that contains a nitrogen-doped bamboo-like carbon nanotube (N-BCNT) on the surface of zeolite [64]. Vanyorek et al. developed a SoS system to improve the effectiveness of aniline production. Examination of various noble metal catalysts has shown that Pt/N-BCNT-zeolite was the most active (at 50 °C, 5 atm). However, in the case of Pd/N-BCNT only one main by-product was formed.

Li et al. prepared and investigated a platinum nanoparticle-containing catalyst with a CMK3 ordered mesoporous carbon support [36]. They examined its catalytic activity for the hydrogenation of nitrobenzene and its derivatives in ethanol. According to the study, the performance of the Pt/CMK-3 catalyst was excellent within a very short time. A reusability test of the catalyst was also done. The Pt/CMK-3 catalyst could be recovered easily, and could be reused more than 14 times with no loss in activity.

Researchers from the University of Miskolc examined another type of catalyst. They prepared a carbonized cellulose catalyst support and used palladium nanoparticles as the active metal for hydrogenation [50]. The temperature dependence of the catalytic reaction was examined. The catalyst developed by Prekob et al. reached 100% conversion at 323 K and 20 atm in 240 min.

Nie et al. synthetized a mesoporous Al_2O_3-supported platinum catalyst [44]. They developed a special, solvent-free, rapid and generalized method for catalyst preparation by ball milling. The catalyst performed well in the selective hydrogenation of nitrobenzene at 40 °C and 20 atm.

The research of Z. Wang et al. yielded a mild, green, and sustainable preparation method of a Pd/CNT catalyst [44]. The focal point of the process is that the implementation occurred in aqueous solution and at room temperature. The catalyst has shown high performance within 15 min under mild conditions. According to the recyclability test, the catalyst could be used three times without demonstrating any loss in activity and selectivity.

Experiments of Dong et al. focused on metallic impurities in carbon nanomaterials [44]. They demonstrated the deactivation effect of residual growth of N-doped carbon nanotubes for hydrogenation. This effect was examined through carbon nanotubes supported by palladium nanoparticles with controllable iron contamination. Only tens of ppm of iron contamination had a significant negative impact on the catalytic performance.

Cerium-oxide is a less commonly used catalyst support. According to a study, cerium-oxide supported platinum catalyst demonstrated a high level of aniline productivity. Q. Zhang et al. studied the effect of the shape of the support and the key role of additional cerium ions sites [62]. The shape effect was attributed to exposed crystal planes on CeO_2 with different reducibility. High temperature reduction has improved the performance of the catalyst by providing additional Ce^{3+} sites on the surface. They prepared Na-containing cerium-oxide support, because they found that Na^+ could help stabilize the Ce^{3+} surface.

Metal-organic frameworks have gained attention in recent years. Du et al. fabricated homogeneously dispersed platinum adatoms in an ordered mesoporous meta-organic framework [65]. Pt@MIL-101 catalysts also demonstrated a high catalytic activity under relatively mild conditions (20 °C and 10 atm). The high efficiency of the catalyst was attributed to the homogeneous deposition of platinum particles in the carrier.

The research of Lv et al. dealt with a preparation of an iron oxide modified, N-doped porous carbon catalyst derived from porous organic polymers [84]. The great advantage of the catalysts is that it can be easily recycled with a magnet and reused at least ten times without reducing the catalytic activity and selectivity, according to the experiments.

Table 4. List of Q1 catalysts according to MIRA21.

RANK	CAT. ID	CAT. Name in Journal	Reference	KNOWN Parameters	MIRA21 Number	Class.
13	HNB_HYD2016_3	Ni/C-Al_2O_3	[61]	15	11.53	Q1
14	HNB_BEI2012_3	Pt/TiO_2/RGO	[64]	14	11.51	Q1
15	HNB_CHE2009_1 *	1 wt% Pd/HT	[60]	14	11.51	Q1
16	HNB_FUY2018_2	PtCo nanoparticle	[55]	14	11.49	Q1
17	HNB_FUY2018_1	PtCo nanoflower	[55]	14	11.47	Q1
18	HNB_BEI2005_2	Pt CNT	[87]	15	11.42	Q1
19	HNB_GUA2017_2	Pd/CNT	[73]	15	11.41	Q1
20	HNB_BEI2012_2	Pt/RGO	[64]	14	11.33	Q1
21	HNB_BEI2005_1	Pt CNT	[87]	15	11.33	Q1
22	HNB_CHE2009_2 *	1 wt% Pd/MgO	[60]	14	11.32	Q1
23	HNB_CHE2009_3 *	1 wt% Pd/Υ-Al_2O_3	[60]	14	11.32	Q1
24	HNB_BEI2013_3	Pd/MWCNT-SA-3.6	[86]	15	11.31	Q1
25	HNB_GUA2017_1	Pd/NCNT	[73]	15	11.30	Q1
26	HNB_BEI2007_3	Pt/CNTs LRT	[75]	15	11.30	Q1
27	HNB_BEI2012_1	Pt/TiO_2	[64]	14	11.29	Q1
28	HNB_BEI2013_1	Pd/MWCNT-SA-6.0	[86]	15	11.28	Q1
29	HNB_GUA2020_2	Pt/CeO2-R	[76]	15	11.26	Q1
30	HNB_BEI2014_1	Pd/Fe_2O_3	[62]	15	11.11	Q1
31	HNB_BEI2008_1	Pd/FSA	[72]	14	11.09	Q1
32	HNB_BEI2013_5	Pd/MWCNT-IM	[86]	15	11.08	Q1
33	HNB_BEI2010_1	5 wt% Pt/MWNT	[74]	14	11.04	Q1
34	HNB_WUH2016_1	C-Fe_3O_4-Pd	[52]	14	10.98	Q1
35	HNB_GUA2020_1	Pt/CeO_2-C	[76]	15	10.96	Q1
36	HNB_BLO2015_7	Ru-14	[68]	14	10.95	Q1
37	HNB_GUA2020_1	Pt CeO_2-R-300	[76]	15	10.91	Q1
38	HNB_TAI2017_2	Co@NMC-700	[89]	15	10.90	Q1
39	HNB_TIA2019_1	Co-NSPC-N	[69]	15	10.90	Q1
40	HNB_INC2018_1	Pd/NH_2-UiO-66	[58]	15	10.87	Q1
41	HNB_BEI2010_2	27.4 wt% Pt/MWNT	[74]	14	10.85	Q1
42	HNB_BEI2010_3	50 wt% Pt/MWNT	[74]	14	10.84	Q1
43	HNB_POR2016_4	50 wt% NiO/Al_2O_3 + SiO_2	[67]	15	10.84	Q1
44	HNB_BEI2007_1	Pt/CNTs HRT	[75]	15	10.83	Q1
45	HNB_POR2016_2	0.3 wt% Pd/Al_2O_3/1.85	[67]	15	10.83	Q1
46	HNB_POR2016_1	1 wt% Pd/Al_2O_3	[67]	15	10.78	Q1
47	HNB_GUA2020_3	Pt/CeO_2-P	[76]	15	10.76	Q1
48	HNB_BLO2015_6	Ru-12	[68]	14	10.72	Q1
49	HNB_BLO2015_5	Ru-7	[68]	14	10.72	Q1
50	HNB_GUA2020_4	Pt CeO2-C-600	[76]	15	10.71	Q1
51	HNB_TAI2017_4	Co@NMC-900	[89]	15	10.70	Q1
52	HNB_GUA2017_3	Pd/CNT	[73]	15	10.67	Q1
53	HNB_BLO2015_3	Ru-5	[68]	14	10.63	Q1
54	HNB_MIS2019_2	Pt/N-BCNT	[51]	14	10.63	Q1
55	HNB_BEI2010_4	10 wt% Pt/C	[74]	14	10.62	Q1

The catalysts tested in the tubular reactor are marked with *.

Table 5. List of Q2 catalysts according to MIRA21.

RANK	CATALYST ID	CAT. Name in Journal	Reference	KNOWN Parameters	MIRA21 Number	Class.
56	HNB_BLO2015_4	Ru-11	[68]	14	10.56	Q2
57	HNB_XIA2019_1	Ni-Zn/AC-350	[97]	15	10.51	Q2
58	HNB_MIS2019_3	Rh/N-BCNT	[51]	14	10.49	Q2
59	HNB_HAN2010_1	Ni-5/SiO_2-EN	[50]	15	10.41	Q2
60	HNB_POR2016_4	50 wt% NiO/Al_2O_3 + SiO_2	[67]	15	10.36	Q2
61	HNB_BEI2013_6	Pd/AC	[86]	14	10.32	Q2
62	HNB_BEI2007_2	Pt/AC HRT	[75]	15	10.31	Q2
63	HNB_BLO2015_2	Ru-16	[86]	14	10.31	Q2
64	HNB_CAR2018_1	AuPd/TiO_2 (MIM)	[91]	14	10.21	Q2
65	HNB_POR2008_1	NiFC1	[56]	14	10.18	Q2
66	HNB_POR2008_2	NiFC2	[56]	14	10.17	Q2
67	HNB_HYD2016_1	Ni/C	[61]	15	10.16	Q2
68	HNB_TIA2019_2	Co-NSPC-C	[69]	15	10.10	Q2
69	HNB_POR2008_3	NiFC3	[56]	14	10.07	Q2
70	HNB_GUA2020_6	Pt CeO_2-P-600	[76]	15	10.05	Q2
71	HNB_BEI2013_4	Pd NPs-4.3	[86]	14	10.04	Q2
72	HNB_WUH2019_1	Co@CN-800	[71]	13	9.99	Q2
73	HNB_TOU2020_1	PdB	[70]	14	9.92	Q2
74	HNB_CAR2018_7	AuPd/TiO_2 (S_{IM})	[91]	14	9.89	Q2
75	HNB_BEI2010_5	5 wt% Pt/C	[74]	14	9.88	Q2
76	HNB_BLO2015_1	Ru-18	[68]	14	9.77	Q2
77	HNB_TAI2017_9	Co@NC@SiO_2-800	[89]	14	9.75	Q2
78	HNB_LAN2020_2	γ-Fe_2O_3/NPC-700	[57]	14	9.70	Q2
79	HNB_TAI2017_12	Co@NMC-800 (1:2)	[89]	13	9.60	Q2
80	HNB_LAN2020_1	γ-Fe_2O_3/NPC-600	[57]	14	9.58	Q2
81	HNB_CAR2018_3	Pd/TiO_2 (M_{IM})	[91]	14	9.56	Q2
82	HNB_TIA2019_3	Co-NSPC-S	[69]	15	9.55	Q2
83	HNB_CHA2016_3	Ni1.99P-s-1 h	[53]	13	9.54	Q2
84	HNB_BEI2017_1	Co_3S_4	[63]	13	9.51	Q2
85	HNB_TOK2004_1	Pt/C 200 °C-2 h	[90]	14	9.47	Q2
86	HNB_TAI2017_5	Co/NMC-800	[89]	13	9.47	Q2
87	HNB_TAI2017_7	Co@NMC-800-H2SO4	[89]	13	9.43	Q2
88	HNB_TAI2017_8	Co@NC-800	[89]	14	9.42	Q2
89	HNB_CAR2018_6	AuPd/TiO_2 (C_{IM})	[91]	14	9.39	Q2
90	HNB_HAR2019_1	FeOx@CN-hpes-400	[54]	13	9.39	Q2
91	HNB_LAN2020_4	γ-Fe_2O_3/NPC-900	[57]	14	9.35	Q2
92	HNB_TOK2004_3	Pt/C 500 °C-2 h	[90]	14	9.35	Q2
93	HNB_TIA2019_4	Co-NSPC-Cl	[69]	15	9.32	Q2
94	HNB_TOK2004_2	Pt/C 300 °C-2 h	[90]	14	9.31	Q2
95	HNB_CAR2018_4	AuPd/MgO (M_{IM})	[91]	14	9.30	Q2
96	HNB_HYD2008_4 *	Ru/SBA-15	[88]	12	9.25	Q2
97	HNB_LAN2020_5	γ-Fe_2O_3/NPC-1000	[57]	14	9.22	Q2
98	HNB_HYD2008_5 *	Ru/SBA-15	[88]	12	9.15	Q2
99	HNB_POR2008_4	RNi	[56]	13	9.12	Q2
100	HNB_HAN2010_4	Ni-15/SiO_2-EN	[50]	13	9.11	Q2
101	HNB_TOK2004_4	Pt/C 600 °C-2 h	[90]	14	9.08	Q2
102	HNB_HYD2008_3 *	Ru/SBA-15	[88]	12	9.03	Q2
103	HNB_CHA2016_2	Ni1.91P-s-0.5 h	[53]	13	8.97	Q2

The catalysts tested in the tubular reactor are marked with *.

Table 6. List of Q3 and Q4 catalysts according to MIRA21.

RANK	CATALYST ID	CAT. Name in Journal	Reference	KNOWN Parameters	MIRA21 Number	Class.
104	HNB_CHA2016_4	Ni2.05P-s-3 h	[53]	13	8.88	Q3
105	HNB_GUA2020_3	Pt CeO_2-C-300	[76]	13	8.88	Q3
106	HNB_NAN2014_1	Pt/AlO(OH)	[80]	11	8.81	Q3
107	HNB_HAN2010_2	Ni-5/SiO_2-NI	[50]	15	8.80	Q3
108	HNB_BEI2007_4	Pt/AC LRT	[75]	15	8.76	Q3
109	HNB_HAN2010_3	Ni-5/SiO_2-AC	[50]	15	8.76	Q3
110	HNB_HAN2010_3	Ni-5/SiO_2-AC	[50]	15	8.75	Q3
111	HNB_CHA2016_1	Ni1.96P-s-10 min	[53]	13	8.69	Q3
112	HNB_TAI2017_1	Co@NMC-600	[89]	14	8.63	Q3
113	HNB_HYD2008_2 *	Ru/SBA-15	[88]	12	8.60	Q3
114	HNB_BEI2005_3	Pt AC	[87]	14	8.50	Q3
115	HNB_BEI2005_1	Cu/SiO_2	[66]	11	8.49	Q3
116	HNB_TAI2017_10	Ni@NMC-800	[89]	13	8.43	Q3
117	HNB_BEI2013_7	Pd/Al_2O_3	[86]	13	8.42	Q3
118	HNB_CAR2018_5	AuPd/C (M_{IM})	[91]	14	8.38	Q3
119	HNB_TOK2004_5	Pt/C 750 °C-3 h	[90]	14	8.38	Q3
120	HNB_TAI2017_6	CoOx@NMC-800	[89]	13	8.26	Q3
121	HNB_XIA2021_2	0.075%Pt/SBA-15	[42]	14	8.17	Q3
122	HNB_GUA2020_5	Pt CeO_2-P-300	[76]	13	8.16	Q3
123	HNB_HAN2010_5	Raney Ni	[50]	13	8.09	Q3
124	HNB_CAR2018_2	Au/TiO_2 (M_{IM})	[91]	14	8.04	Q3
125	HNB_HYD2008_1 *	Ru/SBA-15	[88]	12	7.99	Q3
126	HNB_TAI2017_11	Fe@NMC-800	[89]	13	7.92	Q3
127	HNB_NAN2014_3	Pt/MWCNTs	[80]	10	7.92	Q3
128	HNB_XIA2021_3	0.07%Pt/ZrO_2	[42]	14	7.90	Q3
129	HNB_XIA2021_4	0.09%Pt/γ-Al_2O_3	[42]	14	7.89	Q3
130	HNB_NAN2014_2	Pt/Al_2O_3	[80]	10	7.86	Q3
131	HNB_BEI2013_8	Pd/SiO_2	[86]	13	7.84	Q3
132	HNB_NAN2014_4	Pt/AC	[80]	10	7.80	Q3
133	HNB_GLA2002_3	Pd/CSXU	[81]	10	7.77	Q3
134	HNB_GLA2002_2	Pd/CA1	[81]	10	7.57	Q3
135	HNB_SHA2015_2	Pt/C	[79]	12	7.45	Q3
136	HNB_BEI2013_9	Pd/MgO	[86]	13	7.41	Q3
137	HNB_GLA2002_1	Pd/CN1	[81]	10	7.26	Q4
138	HNB_FUY2018_3	Pt/C	[55]	11	6.97	Q4
139	HNB_SHA2006_1	Meso Ni–B	[84]	9	6.95	Q4
140	HNB_SHA2000_1	Pd-B/SiO_2 (fresh)	[85]	9	6.91	Q4
141	HNB_SHA2000_2	Pd-B/SiO_2 (473 K)	[85]	9	6.91	Q4
142	HNB_DAL2015_1 *	Pd/AM	[82]	11	6.90	Q4
143	HNB_NAN2014_5	Pt/TiO_2	[80]	10	6.90	Q4
144	HNB_SHA2000_3	Pd-B/SiO_2 (673 K)	[85]	9	6.88	Q4
145	HNB_QIN2016_2	Ni-Fe-1/SiO_2	[83]	10	6.77	Q4
146	HNB_QIN2016_3	Ni-Fe-2/SiO_2	[83]	10	6.76	Q4
147	HNB_SHA2000_6	Pd/SiO_2 (fresh)	[85]	9	6.66	Q4
148	HNB_SHA2000_4	Pd-B/SiO_2 (873 K)	[85]	9	6.54	Q4
149	HNB_SHA2000_5	Pd-B/SiO_2 (973 K)	[85]	9	6.48	Q4
150	HNB_SHA2006_2	Regular Ni–B	[84]	9	6.41	Q4
151	HNB_DAL2015_2 *	Pd/CNF/monolith	[82]	11	6.39	Q4
152	HNB_NAN2014_6	Pt/MCM-41	[80]	10	6.34	Q4
153	HNB_SHA2000_7	Pd-B	[83]	8	5.78	Q4
154	HNB_QIN2016_1	Fe/SiO_2	[83]	9	5.71	Q4

The catalysts tested in the tubular reactor are marked with *.

5. Summary and Conclusions

The aim of this work was to demonstrate the operation of the MIRA21 model by examining the catalytic hydrogenation of nitrobenzene. This paper summarizes the general

information about the chosen reaction, describes the MIRA21 ranking model, and compares 154 catalysts from 45 articles published in the last 20 years.

The goal of MIRA21 is to characterize the effectiveness of each catalyst with explicit, objective and minimally distorted numerical data. We derived a mathematical equation comprised of 15 factors to rank the catalysts. According to the literature analysis, we found that 15 parameters were both sufficient and necessary to differentiate between the catalysts. However, due to the possible correlation between the descriptors, revisions to our descriptor system was justified. Outliers were identified during data processing. These outliers significantly affected the scaling and scoring.

Using MIRA21 facilitated the collection of information, because it determined the focus of the articles during the data processing. According to the model, the developed catalysts became more comparable. The ranking helps the researchers work by showing a simple number, which characterizes and evaluates the hydrogenation catalyst. The ranking model can be flexibly applied to other catalytic reactions.

As the results of data processing, we experienced that the information found in articles are difficult to use due to the non-standardized data within them. Unclear wordings do not help the reader understand the main points of the publication. A pivotal point among the attributes describing the catalysts is the TON number. Furthermore, few studies would guide catalyst development on the path of industrial application. Based on the research, exploring knowledge about the sustainability of catalysts is beyond the focus of most research.

The ranking of the catalysts enabled the new development trends and directions to be mapped. According to MIRA21 model, the conclusions of this review about nitrobenzene hydrogenation to aniline are as follows.

Monometallic-supported catalysts are the most suitable for the hydrogenation of nitrobenzene, while bimetallic or multimetallic catalysts did not show any outstanding advantages. However, based on the results of the newest catalysts with the highest MIRA21 number, it can be seen that the metal content of the support has a beneficial effect on the performance of the catalyst (see 1. 7. 10. catalysts in the ranking). It can be also seen that in the case of platinum catalyst, various transition metal oxides promote the hydrogenation properties of platinum. It turned out that small amounts of platinum combined with transition metal oxides can be an effective competitor for palladium-on-carbon catalysts.

Precious metals are most often used for aniline production, especially palladium or platinum, but there are some non-noble metals used as catalysts with excellent activity and selectivity, such as iron and cobalt. The development of novel carbon materials overshadows activated carbon as a catalyst carrier, since application of carbon nanotube carriers became more common due to their good catalytic performance. D1-classified catalysts consist of special compositions such as platinum adatoms in ordered mesoporous metal-organic frameworks or iron oxide modified N-doped porous catalyst derived from porous organic polymer.

As a continuation of our research, we would like to make a publication on the economics of catalysts. As aspect of economics, our work compares for a long time world market price of different precious metal catalysts.

Author Contributions: Conceptualization, A.J.-N., B.V.; methodology, A.J.-N., B.V., E.S., Á.P., M.S. (Martin Szabó), R.Z.B., K.N., M.S. (Milán Szőriand), L.V.; software, K.N., M.S. (Milán Szőriand); writing—original draft preparation, A.J.-N., E.S., Á.P., M.S. (Martin Szabó), L.F., L.V.; writing—review and editing, A.J.-N., L.F., B.V.; supervision, B.V.; funding acquisition, B.V. All authors have read and agreed to the published version of the manuscript.

Funding: This research was supported by the European Union and the Hungarian State, co-financed by the European Regional Development Fund in the framework of the GINOP-2.3.4-15-2016-00004 project, aimed to promote the cooperation between higher education and industry.

Data Availability Statement: A website has been created for the database where all data are available. Website address is https://mira21.iit.uni-miskolc.hu (accessed on 28 March 2022).

Acknowledgments: We thank Tamás Purzsa from Wanhua-BorsodChem for his helpful contributions. We also acknowledge the opportunity provided by Wanhua-BorsodChem to conduct this study. Prepared with the professional support of the Doctoral Student Scholarship Program of the Co-operative Doctoral Program of the Ministry of Innovation and Technology financed from the National Research, Development and Innovation Fund.

Conflicts of Interest: The authors declare no conflict of interest.

References

1. Friend, C.M.; Xu, B. Heterogeneous Catalysis: A Central Science for a Sustainable Future. *Acc. Chem. Res.* **2017**, *50*, 517–521. [CrossRef] [PubMed]
2. Perego, C.; Villa, P. Catalyst preparation methods. *Catal. Today* **1997**, *34*, 281–305. [CrossRef]
3. Mittasch, A.; Frankenburg, W. Early Studies of Multicomponent Catalysts. *Adv. Catal.* **1950**, *2*, 81–104. [CrossRef]
4. Mittasch, A.; Frankenburger, W. The historical development and theory of ammonia synthesis. *J. Chem. Educ.* **1929**, *6*, 2097–2098. [CrossRef]
5. Schlögl, R. Catalytic Synthesis of Ammonia—A "Never-Ending Story"? *Angew. Chem. Int. Ed.* **2003**, *42*, 2004–2008. [CrossRef]
6. Boudart, M. Model catalysts: Reductionism for understanding. *Top. Catal.* **2000**, *13*, 147–149. [CrossRef]
7. Günay, M.E.; Yıldırım, R. Recent advances in knowledge discovery for heterogeneous catalysis using machine learning. *Catal. Rev.* **2021**, *63*, 120–164. [CrossRef]
8. Stanislaus, A.; Cooper, B.H. Aromatic Hydrogenation Catalysis: A Review. *Catal. Rev.* **1994**, *36*, 75–123. [CrossRef]
9. Medford, A.J.; Kunz, M.R.; Ewing, S.M.; Borders, T.; Fushimi, R. Extracting Knowledge from Data through Catalysis Informatics. *ACS Catal.* **2018**, *8*, 7403–7429. [CrossRef]
10. Prezhdo, O.V. Advancing Physical Chemistry with Machine Learning. *J. Phys. Chem. Lett.* **2020**, *11*, 9656–9658. [CrossRef]
11. Dral, P.O. Quantum Chemistry in the Age of Machine Learning. *J. Phys. Chem. Lett.* **2020**, *11*, 2336–2347. [CrossRef] [PubMed]
12. Carleo, G.; Cirac, I.; Cranmer, K.; Daudet, L.; Schuld, M.; Tishby, N.; Vogt-Maranto, L.; Zdeborová, L. Machine learning and the physical sciences. *Rev. Mod. Phys.* **2019**, *91*, 045002. [CrossRef]
13. McCoy, J.; Auret, L. Machine learning applications in minerals processing: A review. *Miner. Eng.* **2019**, *132*, 95–109. [CrossRef]
14. Libbrecht, M.; Noble, W.S. Machine learning applications in genetics and genomics. *Nat. Rev. Genet.* **2015**, *16*, 321–332. [CrossRef]
15. McCullough, K.; Williams, T.; Mingle, K.; Jamshidi, P.; Lauterbach, J. High-throughput experimentation meets artificial intelligence: A new pathway to catalyst discovery. *Phys. Chem. Chem. Phys.* **2020**, *22*, 11174–11196. [CrossRef] [PubMed]
16. Tran, K.; Neiswanger, W.; Broderick, K.; Xing, E.; Schneider, J.; Ulissi, Z.W. Computational catalyst discovery: Active classification through myopic multiscale sampling. *J. Chem. Phys.* **2021**, *154*, 124118. [CrossRef]
17. Williams, T.; McCullough, K.; Lauterbach, J.A. Enabling Catalyst Discovery through Machine Learning and High-Throughput Experimentation. *Chem. Mater.* **2019**, *32*, 157–165. [CrossRef]
18. Takahashi, L.; Ohyama, J.; Nishimura, S.; Takahashi, K. Representing the Methane Oxidation Reaction via Linking First-Principles Calculations and Experiment with Graph Theory. *J. Phys. Chem. Lett.* **2021**, *12*, 558–568. [CrossRef]
19. Takasao, G.; Wada, T.; Thakur, A.; Chammingkwan, P.; Terano, M.; Taniike, T. Machine Learning-Aided Structure Determination for $TiCl_4$–Capped $MgCl_2$ Nanoplate of Heterogeneous Ziegler–Natta Catalyst. *ACS Catal.* **2019**, *9*, 2599–2609. [CrossRef]
20. Li, X.; Chiong, R.; Hu, Z.; Cornforth, D.; Page, A.J. Improved Representations of Heterogeneous Carbon Reforming Catalysis Using Machine Learning. *J. Chem. Theory Comput.* **2019**, *15*, 6882–6894. [CrossRef]
21. Toyao, T.; Maeno, Z.; Takakusagi, S.; Kamachi, T.; Takigawa, I.; Shimizu, K.-I. Machine Learning for Catalysis Informatics: Recent Applications and Prospects. *ACS Catal.* **2019**, *10*, 2260–2297. [CrossRef]
22. Takigawa, I.; Shimizu, K.-I.; Tsuda, K.; Takakusagi, S. Machine Learning Predictions of Factors Affecting the Activity of Heterogeneous Metal Catalysts. In *Nanoinformatics*; Springer: Singapore, 2018; pp. 45–64. [CrossRef]
23. Rothenberg, G. Data mining in catalysis: Separating knowledge from garbage. *Catal. Today* **2008**, *137*, 2–10. [CrossRef]
24. Pirro, L.; Mendes, P.; Paret, S.; Vandegehuchte, B.D.; Marin, G.B.; Thybaut, J.W. Descriptor–property relationships in heterogeneous catalysis: Exploiting synergies between statistics and fundamental kinetic modelling. *Catal. Sci. Technol.* **2019**, *9*, 3109–3125. [CrossRef]
25. SciFinder®, (n.d.). Available online: https://scifinder.cas.org (accessed on 13 April 2022).
26. Global Nitrobenzene Market Size | Industry Report, 2020–2027, (n.d.). Available online: https://www.grandviewresearch.com/industry-analysis/nitrobenzene-market (accessed on 21 June 2021).
27. Nitro Aromatics Market—Global Industry Analysis 2016–2020 and Opportunity Assessment 2021–2031, (n.d.). Available online: https://www.persistencemarketresearch.com/market-research/nitro-aromatics-market.asp (accessed on 25 April 2021).
28. Tafesh, A.M.; Weiguny, J. A Review of the Selective Catalytic Reduction of Aromatic Nitro Compounds into Aromatic Amines, Isocyanates, Carbamates, and Ureas Using CO. *Chem. Rev.* **1996**, *96*, 2035–2052. [CrossRef]
29. Handbook of Heterogeneous Catalytic Hydrogenation for Organic Synthesis | Wiley, (n.d.). Available online: https://www.wiley.com/en-us/Handbook+of+Heterogeneous+Catalytic+Hydrogenation+for+Organic+Synthesis-p-9780471396987 (accessed on 25 April 2021).

30. Aubakirov, Y.; Sassykova, L.; Subramanian, S.; Bhaskar, K.; Otzhan, U.; Amangeldi, M.; Abildin, T.; Zhumakanova, A.; Zhussupova, A.; Zharkyn, M. Hydrogenation of aromatic nitro-compounds of a different structure in a liquid phase. *J. Chem. Technol. Metall.* **2019**, *54*, 522–530.
31. Wegener, G.; Brandt, M.; Duda, L.; Hofmann, J.; Klesczewski, B.; Koch, D.; Kumpf, R.-J.; Orzesek, H.; Pirkl, H.-G.; Six, C.; et al. Trends in industrial catalysis in the polyurethane industry. *Appl. Catal. A Gen.* **2001**, *221*, 303–335. [CrossRef]
32. Kahl, T.; Schröder, K.-W.; Lawrence, F.R.; Marshall, W.J.; Höke, H.; Jäckh, R. *Ullmann's Encyclopedia of Industrial Chemistry*; Wiley-VCH Verlag GmbH & Co. KGaA: Weinheim, Germany, 2000. [CrossRef]
33. Nieto-Márquez, A.; Gil, S.; Romero, A.; Valverde, J.L.; Gómez-Quero, S.; Keane, M.A. Gas phase hydrogenation of nitrobenzene over acid treated structured and amorphous carbon supported Ni catalysts. *Appl. Catal. A Gen.* **2009**, *363*, 188–198. [CrossRef]
34. Turáková, M.; Salmi, T.; Eränen, K.; Wärnå, J.; Murzin, D.Y.; Králik, M. Liquid phase hydrogenation of nitrobenzene. *Appl. Catal. A Gen.* **2015**, *499*, 66–76. [CrossRef]
35. Song, J.; Huang, Z.-F.; Pan, L.; Li, K.; Zhang, X.; Wang, L.; Zou, J.-J. Review on selective hydrogenation of nitroarene by catalytic, photocatalytic and electrocatalytic reactions. *Appl. Catal. B Environ.* **2018**, *227*, 386–408. [CrossRef]
36. Yanji, Z.; Zhou, J. Synergistic catalysis by a hybrid nanostructure Pt catalyst for high-efficiency selective hydrogenation of nitroarenes. *J. Catal.* **2021**, *395*, 445–456.
37. Höller, V.; Wegricht, D.; Yuranov, I.; Kiwi-Minsker, L.; Renken, A. Three-Phase Nitrobenzene Hydrogenation over Supported Glass Fiber Catalysts: Reaction Kinetics Study. *Chem. Eng. Technol.* **2000**, *23*, 251–255. [CrossRef]
38. Burge, H.D.; Collins, D.J.; Davis, B.H. Intermediates in the Raney Nickel Catalyzed Hydrogenation of Nitrobenzene to Aniline. *Ind. Eng. Chem. Prod. Res. Dev.* **1980**, *19*, 389–391. [CrossRef]
39. Figueras, F.; Coq, B. Hydrogenation and hydrogenolysis of nitro-, nitroso-, azo-, azoxy- and other nitrogen-containing compounds on palladium. *J. Mol. Catal. A Chem.* **2001**, *173*, 223–230. [CrossRef]
40. Gelder, E.A.; Jackson, S.D.; Lok, C.M. The hydrogenation of nitrobenzene to aniline: A new mechanism. *Chem. Commun.* **2004**, 522–524. [CrossRef] [PubMed]
41. Mahata, A.; Rai, R.K.; Choudhuri, I.; Singh, S.K.; Pathak, B. Direct vs. indirect pathway for nitrobenzene reduction reaction on a Ni catalyst surface: A density functional study. *Phys. Chem. Chem. Phys.* **2014**, *16*, 26365–26374. [CrossRef]
42. Fayyad, U.; Piatetsky-shapiro, G.; Smyth, P. From data mining to knowledge discovery in databases. *AI Mag.* **1996**, *17*, 37–54. [CrossRef]
43. Neeli, C.K.P.; Puthiaraj, P.; Lee, Y.-R.; Chung, Y.-M.; Baeck, S.-H.; Ahn, W.-S. Transfer hydrogenation of nitrobenzene to aniline in water using Pd nanoparticles immobilized on amine-functionalized UiO-66. *Catal. Today* **2018**, *303*, 227–234. [CrossRef]
44. Nie, S.; Yang, S.; Zhang, P. Solvent-free synthesis of mesoporous platinum-aluminum oxide via mechanochemistry: Toward selective hydrogenation of nitrobenzene to aniline. *Chem. Eng. Sci.* **2020**, *220*, 115619. [CrossRef]
45. Sangeetha, P.; Shanthi, K.; Rao, K.R.; Viswanathan, B.; Selvam, P. Hydrogenation of nitrobenzene over palladium-supported catalysts—Effect of support. *Appl. Catal. A Gen.* **2009**, *353*, 160–165. [CrossRef]
46. Venkateshwarlu, V.; Mohan, V.; Rao, M.V.; Nagaiah, P.; Raju, B.D.; Rao, K.R. Advantage of carbon coverage over Al2O3 as support for Ni/C-Al2O3 catalyst in vapour phase hydrogenation of nitrobenzene to aniline. *Catal. Commun.* **2016**, *86*, 1–4. [CrossRef]
47. Wang, Y.; Deng, Y.; Shi, F. Active palladium catalyst preparation for hydrogenation reactions of nitrobenzene, olefin and aldehyde derivatives. *J. Mol. Catal. A Chem.* **2014**, *395*, 195–201. [CrossRef]
48. Xu, Y.; Lv, X.-J.; Chen, Y.; Fu, W.-F. Highly selective reduction of nitroarenes to anilines catalyzed using MOF-derived hollow Co3S4 in water under ambient conditions. *Catal. Commun.* **2017**, *101*, 31–35. [CrossRef]
49. Zhao, Y.; Zhang, H.; Huang, C.; Chen, S.; Liu, Z. Pt/titania/reduced graphite oxide nanocomposite: An efficient catalyst for nitrobenzene hydrogenation. *J. Colloid Interface Sci.* **2012**, *374*, 83–88. [CrossRef] [PubMed]
50. Prekob, A.; Hajdu, V.; Muránszky, G.; Fiser, B.; Sycheva, A.; Ferenczi, T.; Viskolcz, B.; Vanyorek, L. Application of carbonized cellulose-based catalyst in nitrobenzene hydrogenation. *Mater. Today Chem.* **2020**, *17*, 100337. [CrossRef]
51. Diao, S.; Qian, W.; Luo, G.; Wei, F.; Wang, Y. Gaseous catalytic hydrogenation of nitrobenzene to aniline in a two-stage fluidized bed reactor. *Appl. Catal. A Gen.* **2005**, *286*, 30–35. [CrossRef]
52. Couto, C.S.; Madeira, L.M.; Nunes, C.P.; Araújo, P. Commercial catalysts screening for liquid phase nitrobenzene hydrogenation. *Appl. Catal. A Gen.* **2016**, *522*, 152–164. [CrossRef]
53. Wang, J.; Yuan, Z.; Nie, R.; Hou, Z.; Zheng, X. Hydrogenation of Nitrobenzene to Aniline over Silica Gel Supported Nickel Catalysts. *Ind. Eng. Chem. Res.* **2010**, *49*, 4664–4669. [CrossRef]
54. Easterday, R.; Sanchez-Felix, O.; Losovyj, Y.; Pink, M.; Stein, B.D.; Morgan, D.G.; Rakitin, M.; Doluda, V.Y.; Sulman, M.G.; Mahmoud, W.E.; et al. Design of ruthenium/iron oxide nanoparticle mixtures for hydrogenation of nitrobenzene. *Catal. Sci. Technol.* **2015**, *5*, 1902–1910. [CrossRef]
55. Gao, R.; Guo, H.; Wang, B.; Qiu, P.; Sun, M.; Chen, L. Co based N, S co-doped carbon hybrids for catalytic hydrogenation: Role of cobalt salt and doped S. *Appl. Catal. A Gen.* **2019**, *579*, 99–105. [CrossRef]
56. Garg, G.; Foltran, S.; Favier, I.; Pla, D.; Medina-González, Y.; Gómez, M. Palladium nanoparticles stabilized by novel choline-based ionic liquids in glycerol applied in hydrogenation reactions. *Catal. Today* **2020**, *346*, 69–75. [CrossRef]
57. Hu, A.; Lu, X.; Cai, D.; Pan, H.; Jing, R.; Xia, Q.; Zhou, D.; Xia, Y. Selective hydrogenation of nitroarenes over MOF-derived Co@CN catalysts at mild conditions. *Mol. Catal.* **2019**, *472*, 27–36. [CrossRef]

58. Lang, Y.; Wang, Q.; Xing, J.; Zhang, B.; Liu, H. Preparation of magnetic γ-Al_2O_3supported palladium catalyst for hydrogenation of nitrobenzene. *AIChE J.* **2008**, *54*, 2303–2309. [CrossRef]
59. Dong, B.; Li, Y.; Ning, X.; Wang, H.; Yu, H.; Peng, F. Trace iron impurities deactivate palladium supported on nitrogen-doped carbon nanotubes for nitrobenzene hydrogenation. *Appl. Catal. A Gen.* **2017**, *545*, 54–63. [CrossRef]
60. Sun, Z.; Zhao, Y.; Xie, Y.; Tao, R.; Zhang, H.; Huang, C.; Liu, Z. The solvent-free selective hydrogenation of nitrobenzene to aniline: An unexpected catalytic activity of ultrafine Pt nanoparticles deposited on carbon nanotubes. *Green Chem.* **2010**, *12*, 1007–1011. [CrossRef]
61. Zhao, Y.; Li, C.-H.; Yu, Z.-X.; Yao, K.-F.; Ji, S.-F.; Liang, J. Effect of microstructures of Pt catalysts supported on carbon nanotubes (CNTs) and activated carbon (AC) for nitrobenzene hydrogenation. *Mater. Chem. Phys.* **2007**, *103*, 225–229. [CrossRef]
62. Zhang, Q.; Bu, J.-H.; Wang, J.; Sun, C.; Zhao, D.; Sheng, G.; Xie, X.; Sun, M.; Yu, L. Highly Efficient Hydrogenation of Nitrobenzene to Aniline over Pt/CeO_2 Catalysts: The Shape Effect of the Support and Key Role of Additional Ce^{3+} Sites. *ACS Catal.* **2020**, *10*, 10350–10363. [CrossRef]
63. Huang, L.; Lv, Y.; Wu, S.; Liu, P.; Xiong, W.; Hao, F.; Luo, H. Activated carbon supported bimetallic catalysts with combined catalytic effects for aromatic nitro compounds hydrogenation under mild conditions. *Appl. Catal. A Gen.* **2019**, *577*, 76–85. [CrossRef]
64. Vanyorek, L.; Prekob, A.; Sikora, E.; Reizer, E.; Muránszky, G.; Kristály, F.; Viskolcz, B.; Fiser, B. Application of carbon nanotube coated aluminosilicate beads as "support on support" catalyst for hydrogenation of nitrobenzene. *J. Ind. Eng. Chem.* **2019**, *79*, 307–313. [CrossRef]
65. Du, W.; Chen, G.; Nie, R.; Li, Y.; Hou, Z. Highly dispersed Pt in MIL-101: An efficient catalyst for the hydrogenation of nitroarenes. *Catal. Commun.* **2013**, *41*, 56–59. [CrossRef]
66. Li, J.; Li, X.; Ding, Y.; Wu, P. Pt nanoparticles entrapped in ordered mesoporous carbons: An efficient catalyst for the liquid-phase hydrogenation of nitrobenzene and its derivatives. *Chin. J. Catal.* **2015**, *36*, 1995–2003. [CrossRef]
67. Fan, G.; Wang, Y.; Wang, C. One-pot synthesis of aluminum oxyhydroxide matrix-entrapped Pt nanoparticles as an excellent catalyst for the hydrogenation of nitrobenzene. *RSC Adv.* **2014**, *4*, 10997–11002. [CrossRef]
68. Gelder, E.A.; Jackson, S.D.; Lok, C.M. A Study of Nitrobenzene Hydrogenation Over Palladium/Carbon Catalysts. *Catal. Lett.* **2002**, *84*, 205–208. [CrossRef]
69. Du, B.; Su, H.; Wang, S. Palladium supported on carbon nanofiber coated monoliths for three-phase nitrobenzene hydrogenation: Influence of reduction temperature and oxidation pre-treatment. *J. Ind. Eng. Chem.* **2015**, *21*, 997–1004. [CrossRef]
70. Sun, X.; Du, F. Synthesis and higher catalytic property of the novel bimetallic Ni–Fe/SiO2 microspheres with mesoporous structure. *J. Mater. Res.* **2017**, *32*, 766–774. [CrossRef]
71. Li, H.; Zhao, Q.; Wan, Y.; Dai, W.; Qiao, M. Self-assembly of mesoporous Ni–B amorphous alloy catalysts. *J. Catal.* **2006**, *244*, 251–254. [CrossRef]
72. Yu, X.; Wang, M.; Li, H. Study on the nitrobenzene hydrogenation over a Pd-B/SiO2 amorphous catalyst. *Appl. Catal. A Gen.* **2000**, *202*, 17–22. [CrossRef]
73. Wang, Z.; Liu, H.; Chen, L.; Chou, L.; Wang, X. Green and facile synthesis of carbon nanotube supported Pd nanoparticle catalysts and their application in the hydrogenation of nitrobenzene. *J. Mater. Res.* **2013**, *28*, 1326–1333. [CrossRef]
74. Li, C.-H.; Yu, Z.-X.; Yao, K.-F.; Ji, S.-F.; Liang, J. Nitrobenzene hydrogenation with carbon nanotube-supported platinum catalyst under mild conditions. *J. Mol. Catal. A Chem.* **2005**, *226*, 101–105. [CrossRef]
75. Zhou, P.; Li, D.; Jin, S.; Chen, S.; Zhang, Z. Catalytic transfer hydrogenation of nitro compounds into amines over magnetic graphene oxide supported Pd nanoparticles. *Int. J. Hydrogen Energy* **2016**, *41*, 15218–15224. [CrossRef]
76. Chary, K.V.R.; Srikanth, C.S. Selective Hydrogenation of Nitrobenzene to Aniline over Ru/SBA-15 Catalysts. *Catal. Lett.* **2009**, *128*, 164–170. [CrossRef]
77. Zhang, F.; Zhao, C.; Chen, S.; Li, H.; Yang, H.; Zhang, X.-M. In situ mosaic strategy generated Co-based N-doped mesoporous carbon for highly selective hydrogenation of nitroaromatics. *J. Catal.* **2017**, *348*, 212–222. [CrossRef]
78. Zhao, F.; Ikushima, Y.; Arai, M. Hydrogenation of nitrobenzene with supported platinum catalysts in supercritical carbon dioxide: Effects of pressure, solvent, and metal particle size. *J. Catal.* **2004**, *224*, 479–483. [CrossRef]
79. Qu, R.; Macino, M.; Iqbal, S.; Gao, X.; He, Q.; Hutchings, G.J.; Sankar, M. Supported Bimetallic AuPd Nanoparticles as a Catalyst for the Selective Hydrogenation of Nitroarenes. *Nanomaterials* **2018**, *8*, 690. [CrossRef] [PubMed]
80. Liu, P.; Chang, W.-T.; Liang, X.-Y.; Wang, J.; Li, Y.-X. Small amorphous and crystalline Ni–P particles synthesized in glycol for catalytic hydrogenation of nitrobenzene. *Catal. Commun.* **2016**, *76*, 42–45. [CrossRef]
81. Li, X.; Qi, T.; Wang, J.; She, W.; Mao, G.; Yan, P.; Li, W.; Li, G. Enhanced catalytic performance of nitrogen-doped carbon supported FeOx-based catalyst derived from electrospun nanofiber crosslinked N, Fe-containing MOFs for efficient hydrogenation of nitroarenes. *Mol. Catal.* **2019**, *477*, 110544. [CrossRef]
82. Miao, H.; Hu, S.; Ma, K.; Sun, L.; Wu, F.; Wang, H.; Li, H. Synthesis of PtCo nanoflowers and its catalytic activity towards nitrobenzene hydrogenation. *Catal. Commun.* **2018**, *109*, 33–37. [CrossRef]
83. Mahata, N.; Cunha, A.F.; Órfão, J.; Figueiredo, J. Hydrogenation of nitrobenzene over nickel nanoparticles stabilized by filamentous carbon. *Appl. Catal. A Gen.* **2008**, *351*, 204–209. [CrossRef]
84. Lv, J.; Liu, Z.; Dong, Z. Iron oxide modified N-doped porous carbon derived from porous organic polymers as a highly-efficient catalyst for reduction of nitroarenes. *Mol. Catal.* **2020**, *498*, 111249. [CrossRef]

85. OriginLab—Origin and OriginPro—Data Analysis and Graphing Software, (n.d.). Available online: https://www.originlab.com/ (accessed on 5 May 2021).
86. Costentin, C.; Drouet, S.; Robert, M.; Savéant, J.-M. Turnover Numbers, Turnover Frequencies, and Overpotential in Molecular Catalysis of Electrochemical Reactions. Cyclic Voltammetry and Preparative-Scale Electrolysis. *J. Am. Chem. Soc.* **2012**, *134*, 11235–11242. [CrossRef]
87. Umpierre, A.P.; de Jesús, E.; Dupont, J. Turnover Numbers and Soluble Metal Nanoparticles. *ChemCatChem* **2011**, *3*, 1413–1418. [CrossRef]
88. Kozuch, S.; Martin, J.M.L. "Turning Over" Definitions in Catalytic Cycles. *ACS Catal.* **2012**, *2*, 2787–2794. [CrossRef]
89. Boudart, M.; Aldag, A.; Benson, J.; Dougharty, N.; Harkins, C.G. On the specific activity of platinum catalysts. *J. Catal.* **1966**, *6*, 92–99. [CrossRef]
90. Cornils, B.; Herrmann, W.A.; Wong, C.; Zanthoff, H. (Eds.) *Catalysis from A to Z*; Wiley: Hoboken, NJ, USA, 2013. [CrossRef]
91. Suttiponparnit, K.; Jiang, J.; Sahu, M.; Suvachittanont, S.; Charinpanitkul, T.; Biswas, P. Role of Surface Area, Primary Particle Size, and Crystal Phase on Titanium Dioxide Nanoparticle Dispersion Properties. *Nanoscale Res. Lett.* **2010**, *6*, 27. [CrossRef] [PubMed]
92. Brinkmann, A.; Chen, M.; Couillard, M.; Jakubek, Z.; Leng, T.; Johnston, L.J. Correlating Cellulose Nanocrystal Particle Size and Surface Area. *Langmuir* **2016**, *32*, 6105–6114. [CrossRef]
93. Rioux, R.M.; Song, H.; Hoefelmeyer, J.D.; Yang, A.P.; Somorjai, G.A. High-Surface-Area Catalyst Design: Synthesis, Characterization, and Reaction Studies of Platinum Nanoparticles in Mesoporous SBA-15 Silica. *J. Phys. Chem. B* **2005**, *109*, 2192–2202. [CrossRef]
94. Ganesan, P. Particle size distribution function of supported metal catalysts by X-ray diffraction. *J. Catal.* **1978**, *52*, 310–320. [CrossRef]
95. Matyi, R.J.; Schwartz, L.H.; Butt, J.B. Particle Size, Particle Size Distribution, and Related Measurements of Supported Metal Catalysts. *Catal. Rev.* **1987**, *29*, 41–99. [CrossRef]
96. Datye, A.K.; Xu, Q.; Kharas, K.C.; McCarty, J.M. Particle size distributions in heterogeneous catalysts: What do they tell us about the sintering mechanism? *Catal. Today* **2006**, *111*, 59–67. [CrossRef]
97. Scimago Journal & Country Rank, (n.d.). Available online: https://www.scimagojr.com/ (accessed on 5 May 2021).
98. Bethune, D.S.; Kiang, C.H.; De Vries, M.S.; Gorman, G.; Savoy, R.; Vazquez, J.; Beyers, R. Cobalt-catalysed growth of carbon nanotubes with single-atomic-layer walls. *Nature* **1993**, *363*, 605–607. [CrossRef]
99. Iijima, S.; Ichihashi, T. Single-shell carbon nanotubes of 1-nm diameter. *Nature* **1993**, *363*, 603–605. [CrossRef]
100. Serp, P. Carbon nanotubes and nanofibers in catalysis. *Appl. Catal. A Gen.* **2003**, *253*, 337–358. [CrossRef]
101. Hareesh, H.N.; Minchitha, K.U.; Venkatesh, K.; Nagaraju, N.; Kathyayini, N. Environmentally benign selective hydrogenation of α,β-unsaturated aldehydes and reduction of aromatic nitro compounds using Cu based bimetallic nanoparticles supported on multiwalled carbon nanotubes and mesoporous carbon. *RSC Adv.* **2016**, *6*, 82359–82369. [CrossRef]
102. Tomkins, P.; Gebauer-Henke, E.; Leitner, W.; Müller, T.E. Concurrent Hydrogenation of Aromatic and Nitro Groups over Carbon-Supported Ruthenium Catalysts. *ACS Catal.* **2014**, *5*, 203–209. [CrossRef]
103. Göksu, H.; Zengin, N.; Burhan, H.; Cellat, K.; Şen, F. A Novel Hydrogenation of Nitroarene Compounds with Multi Wall Carbon Nanotube Supported Palladium/Copper Nanoparticles (PdCu@MWCNT NPs) in Aqueous Medium. *Sci. Rep.* **2020**, *10*, 8043. [CrossRef]